Gondwana Research 27 (2015) 38–63

Contents lists available at ScienceDirect

Gondwana Research

journal homepage: www.elsevier.com/locate/gr

GR focus review

Late Cretaceous plume-induced subduction initiation along the southern margin of the Caribbean and NW South America: The first documented example with implications for the onset of plate tectonics

Scott A. Whattam [a,*], Robert J. Stern [b]

[a] Department of Earth and Environmental Sciences, Korea University, Seoul 136-701, Republic of Korea
[b] Geosciences Department, University of Texas at Dallas, Richardson, TX 75083-0688, USA

ARTICLE INFO

Article history:
Received 8 February 2014
Received in revised form 19 July 2014
Accepted 19 July 2014
Available online 23 August 2014

Handling Editor: T. Gerya

Keywords:
Mantle plume
Subduction initiation
Volcanic arc
Caribbean
South America

ABSTRACT

Plate tectonics is the governing theory that unifies the Earth Sciences and is unique to Earth. The sinking of lithosphere in subduction zones drives plate tectonics but exactly how and why subduction begins (subduction initiation, SI) remains enigmatic. Most SI models require exploitation of existing lithospheric weaknesses but these are now produced by plate tectonics; so how did the first subduction zones form? One possibility is SI along a plume head-cold lithosphere interface, but no examples have been documented. On the basis of three key observations, we show here that the Late Cretaceous tectonic evolution of Central America, NW South America and the Leeward Antilles is consistent with plume-induced SI (PISI) which nucleated along the southern and western margins of the Caribbean Plate (Caribbean Large Igneous Province, CLIP) at ~100 Ma. (1) Trace element chemistry of most 100 Ma and younger units interpreted as CLIP that are exposed along the southern margin of the Caribbean Plate and NW South America, record subduction additions which increased with time beginning at 100 Ma. These 'plume- and arc-related' (PAR) units are distinguishable from: (a) global oceanic plateau basalts (OPB); (b) 140–110 Ma OPB along the western edge of the CLIP; and (c) post-100 Ma OPB in the northernmost CLIP. Whereas the older OPB are compositionally identical to global OPB, the younger northerly CLIP units are similar to oceanic island basalts and record lower degrees of partial melting than PAR units exposed along the southern and western peripheries of the CLIP. Both the older and the younger northerly CLIP units lack evidence of subduction modification. (2) There is no known hiatus between CLIP and younger arc units, suggesting continuous tectono-magmatic evolution from plume to arc. (3) Generation of the CLIP and earliest, overlying and crosscutting arc units overlaps in time, space, chemical and isotopic compositions; both units are consistent with derivation from Galapagos Plume-like mantle which became increasingly subduction-modified with time. These observations illustrate that formation of the CLIP and earliest arc volcanism reflects partial melting of the same hybrid plume-subduction-modified source in a single, rapidly evolving tectonic environment. The scale of Late Cretaceous PISI in the SW Caribbean realm is consistent with the expected large scale of lithospheric collapse as seen for other SI examples, extending some 1400 km from southern Costa Rica–Panama to western Colombia and 1700 km from Ecuador to the Leeward Antilles (Aruba and Curaçao). This first documented example of PISI may be relevant to the start of plate tectonics which may have started when subduction began around Precambrian plume heads. Establishment of lava chemostratigraphy designed to establish the composition of early SI magmatic successions might provide keys for deciphering whether SI occurred along a collapsed transform (like the IBM arc; early MORB-like lavas) or around a mantle plume (like the Caribbean; early plateau-like lavas). Recognition of this first example of PISI further suggests that interaction of a sufficiently large plume head with sufficiently dense oceanic lithosphere in Precambrian time may have triggered the modern regime of plate tectonics.

Contents

* Corresponding author. Tel.: +82 2 3290 3172; fax: +82 2 3290 3189.
E-mail address: whattam@korea.ac.kr (S.A. Whattam).

http://dx.doi.org/10.1016/j.gr.2014.07.011
1342-937X/

1. Introduction

Subduction zones return old, cold, oceanic lithosphere to the deep mantle and generate distinctive arc magmas. However, exactly how and why subduction initiation (SI) (see Table 1 for a list of abbreviations used and their definitions) occurs remains controversial. It is contentious whether SI requires a priori convergence (e.g., McKenzie, 1977; Gurnis et al., 2004) or can occur spontaneously (due to collapse of dense lithosphere above underlying asthenosphere, Kemp and Stevenson, 1996; Stern, 2004; Mart et al., 2005; Nikolaeva et al., 2010). Attempted subduction of buoyant lithosphere (e.g., with thick crust) can lead to collision-induced SI (e.g., Cloos, 1993) as in the case of the Miocene Solomon Arc system where collision of the Ontong Java Plateau shut down the south-dipping subduction zone and induced a new north-dipping subduction zone on the south side of the arc (Cooper and Taylor, 1985). This is an example of induced nucleation of a subduction zone (INSZ), reflecting continued plate convergence to form a new subduction zone (Stern, 2004) as reproduced by geodynamic models (e.g., Hall et al., 2003). It is also possible that new subduction zones can form without pre-existing convergence as in the case of spontaneous nucleation of a subduction zone (SNSZ; Stern, 2004). Recent results from geodynamic modeling suggest that SNSZ is also possible (Dymkova and Gerya, 2013). For both INSZ and SNSZ, a pre-existing lithospheric weakness is required to overcome the great strength of oceanic lithosphere, for example a transform fault (Casey and Dewey, 1984; Stern, 2004) or fossil spreading center (Casey and Dewey, 1984).

A better understanding of how new subduction zones form today is also relevant to the question of how the modern regime of plate tectonics began on Earth (see summary in Korenaga, 2013). Because most of the force driving plate motions today results from the sinking of dense lithosphere in subduction zones (Lithgow-Berelloni and Richards, 1995), the question of how plate tectonics began largely depends on understanding how the first subduction zone formed. Addressing this question requires understanding how large-scale lithospheric weaknesses formed in the absence of plate tectonics. Lithospheric weaknesses such as transform faults formed during Phanerozoic time have been generated by plate tectonics, but how did lithospheric weaknesses form prior to the inception of plate tectonics? Recognition of the SW Caribbean as the first plausible PISI example further suggests that a similar mechanism may have been responsible for making the first subduction zone in Precambrian time. Interaction of a sufficiently large plume head with sufficiently dense oceanic lithosphere could have caused the lithospheric weakness that formed the first subduction zones and catalyzed the modern episode of plate tectonics.

In spite of it being simple and plausible, PISI is not widely considered an important way that new subduction zones form. The early suggestion of Niu et al. (2003) that subduction could initiate along the periphery of an oceanic plateau finds support from numerical models (Ueda et al., 2008; Burov and Cloetingh, 2010). Perhaps the most important reason that the hypothesis has not gained wider currency is that until now no convincing examples of PISI have been identified in the rock record. In this paper, we demonstrate that the Late Cretaceous tectonic evolution of Central America and NW South America is consistent with a PISI model. It is widely recognized that subduction in this region began around the southern and western margins of the Caribbean Large Igneous Province oceanic plateau (hereafter referred to as CLIP), but the transformation from plume activity to form the CLIP and subduction to generate younger arc igneous activity is poorly understood. We compile published geochemical and geochronological data to show that the general outlines of a PISI model explain some otherwise enigmatic features of the Late Cretaceous tectonic evolution of the Caribbean Plate.

2. Oceanic plateau- and arc-related oceanic units in Central America and NW South America

Oceanic plateaus (OP) are large mafic igneous provinces comprising oceanic crust that is much thicker than the 5–7 km formed by normal seafloor spreading (Condie and Abbott, 1999). OP form when a mantle plume head – or other large-scale asthenospheric upwelling – ruptures the lithosphere and erupts voluminous basalt. These outpourings are often referred to as Large Igneous Provinces (LIP). Oceanic crust of the Caribbean Plate is often 15–20 km thick (Bowland and Rosencrantz, 1988) and is widely interpreted as an OP that formed above the Galapagos Plume before drifting into the gap between North and South America where it was captured to make up the Caribbean Plate (e.g., Kerr et al., 2000).

Table 1
Abbreviations and definitions.

Abbreviation/ acronym	Definition
AB	Aruba Bathoith
AF	Amaime Formation (Western Cordillera, western Colombia)
AQB	Antioquia Batholith (Central Cordillera, western Colombia)
ALF	Aruba Lava Formation
AP	Azuero Plateau
BB	Buga Batholith (Western Cordillera, western Colombia)
BCC	bulk continental crust
BF	Barrosso Formation (Western Cordillera, western Colombia)
BUC	Bólivar Ultramafic Complex (Colombia)
CBA	Chagres–Bayano Arc (eastern Panama)
CAVA	(modern) Central American Volcanic Arc
CAVAB	(modern) Central American Volcanic Arc basalt
CC	Central Cordillera (of western Colombia)
CD	Curaçao Diorites
CDVC	Cabo de la Vela Complex (Guajira peninsula, northernmost Colombia)
CLIP	Caribbean Large Igneous Province (an OP)
CLF	Curaçao Lava Formation
DSDP	Deep Sea Drilling Project
GAA	Golfito Arc (southern Costa Rica)
GAA	Greater Antilles Arc
HFSE	high-field strength elements (e.g., Nb, Zr, Ti)
IBM	Izu-Bonin–Mariana (a convergent margin in the western Pacific)
IBMVA	modern IBM volcanic arc
INSZ	induced nucleation of subduction zone
LIP	Large Igneous Province (thought to form when mantle plume impinges base of the lithosphere)
MORB	Mid-ocean ridge basalt (pure asthenospheric melt)
NC	Nicoya Complex (western Costa Rica)
ODP	Oceanic Drilling Project
OIB	Ocean island basalt (tholeiitic and alkalic basalts of within-plate oceanic volcanoes)
OP	Oceanic plateau
OPB	Oceanic plateau basalt (plume basalt)
PAR	plume- and arc-related
PG	Pujilí Granite (western Ecuador)
PISI	plume-induced subduction initiation
PU	Pallatanga Unit (western Ecuador)
RCA	Rio Cala Arc (western Ecuador)
SAA	Sona–Azuero Arc (southern Panama)
SDB	Serranía de Baudó (complex, Western Cordillera, western Colombia)
SI	subduction initiation
SIRO	subduction initiation rule ophiolites (e.g., SSZ ophiolites)
SNSZ	spontaneous nucleation of subduction zone
SSZ	spra-subduction zone; i.e. formation in a forearc, arc, or backarc basin, above a subduction zone
THI	tholeiitic index: tholeiitic suites have THI >1; calc-alkaline suites have THI < 1
Tr1	PISI trace 1
Tr2	PISI trace 2
Tr3	PISI trace 3 or eastern
VAB	Volcanic arc basalt (subduction-modified basalt)
VF	Volcanic Formation (western Cordillera,western Colombia)

Whattam and Stern (2004)

Although most of the CLIP is submerged beneath the Caribbean Sea, many Late Cretaceous igneous complexes in Central America (Costa Rica and Panama), NW South America (Colombia and Ecuador) and the southern Caribbean (Aruba and Curaçao, Leeward Antilles) (Fig. 1) are interpreted as CLIP fragments (see references in Table 2). Basal units and sometimes all of these basaltic sequences are interpreted as uplifted or accreted CLIP (Fig. 2). Early studies suggest that the CLIP was mostly constructed between 92 and 88 Ma with minor magmatic pulses at 124–112 Ma and 76–72 Ma (Sinton et al., 1998; Kerr et al., 2003 and references therein) but some later studies (e.g., Serrano et al., 2011) emphasize an extended period of essentially uninterrupted magmatic activity spanning the entire Cretaceous.

We show below that there were two main phases of distinct plateau construction at 140–110 Ma and after 100 Ma and that post-100 Ma OPB-related lavas along the southern margins of the Caribbean Plate and NW South America are compositionally distinct from those of the pre-110 Ma plateau and post-100 Ma plateau units in the central and northerly segments of the plate. Whereas pre-110 Ma and post-100 Ma igneous activity in the center and northerly sections of the Caribbean Plate entailed plume-magmatism only, post 100-Ma magmatism along the southern periphery of the Caribbean Plate and NW South America was a hybrid of plume and subduction zone contributions. Late Cretaceous igneous rocks are common in NW Costa Rica in the west to western Ecuador in the south to the Leeward Antilles in the east. They are also exposed in southern Hispaniola and have been drilled in the middle of the Caribbean Sea. Evidence of subduction contributions disappears along northernmost NW South America (i.e., western Colombia) and the Leeward Antilles at 70–65 Ma, coincident with proposed NW South America–forearc collision at 73–70 Ma and emplacement of OP units eastwards upon South America above a west-dipping subduction zone (Vallejo et al., 2009).

Because there are no obvious breaks between the end of plume magmatism and the beginning of arc magmatism, we use the term 'plume and arc-related' (PAR) units to refer to Late Cretaceous igneous sequences interpreted by other researchers as having formed during this post-100 Ma hybrid igneous environment. We identify three coterminous PISI traces defined by PAR sequences exposed in Central America (Tr1), coastal Colombia and Ecuador (Tr2), and in the Leeward Antilles (Tr3; Fig. 1). Each of these traces is ~1000 km long and each preserves geochemical evidence of plume magmatism evolving into subduction-related magmatism with time. Our goal is to elucidate how the CLIP and the three 1000-km long traces evolved to the modern arc that now occupies Central America and Ecuador–Colombia. All workers who have considered this evolution agree that the transition to arc magmatism began sometime in the Late Cretaceous but disagree about exactly when. In Panama and SE-most Costa Rica, Buchs et al. (2010) identified depletion of high field strength elements (HFSE) and concluded that arc igneous activity began by 75 Ma. In western Ecuador, Vallejo et al. (2009) used a similar argument to conclude that arc igneous activity began by 85 Ma. In Aruba and Curaçao, Wright and Wyld (2011) interpreted the beginning of arc igneous activity as the intrusion of the oldest granitoids dated at 89 Ma. These inferences for the timing of SI in these regions form the basis of our designations of PISI traces (Tr1, Tr2, Tr3, Figs. 1, 2).

Part of the uncertainty in interpreting when the switch from plume to arc magmatism occurred reflects an assumption that the three traces evolved independently, which could be falsified if these three traces are all related to the same plume-to-arc tectonomagmatic transition. The uncertainty of the transition is also reflected in reinterpretation of Central American PAR units as having arc affinities for some sequences previously thought to be CLIP fragments (Wörner et al., 2009; Buchs et al., 2010; Wegner et al., 2011). Stratigraphic relations between plateau and arc units are generally conformable where these can be examined (e.g., western Ecuador, Vallejo et al., 2009; Panama, Buchs et al., 2010) and not separated by any documented unconformity or sedimentary interval (Fig. 2). We take this to indicate that magma sources evolved from plume- to subduction-related without interruption. In the following sections we use geochemical approaches to examine this transition in greater detail.

3. Materials and methods

Below we summarize how we compiled geochemical and age data for our study. Further details of geochemical and geochronological data and tectonic interpretations are provided in the GR Online Supplementary Document.

3.1. Caribbean data compilation

We compiled geochemical, geochronological and isotopic data from southern Central and NW South American PAR complexes (Figs. 1

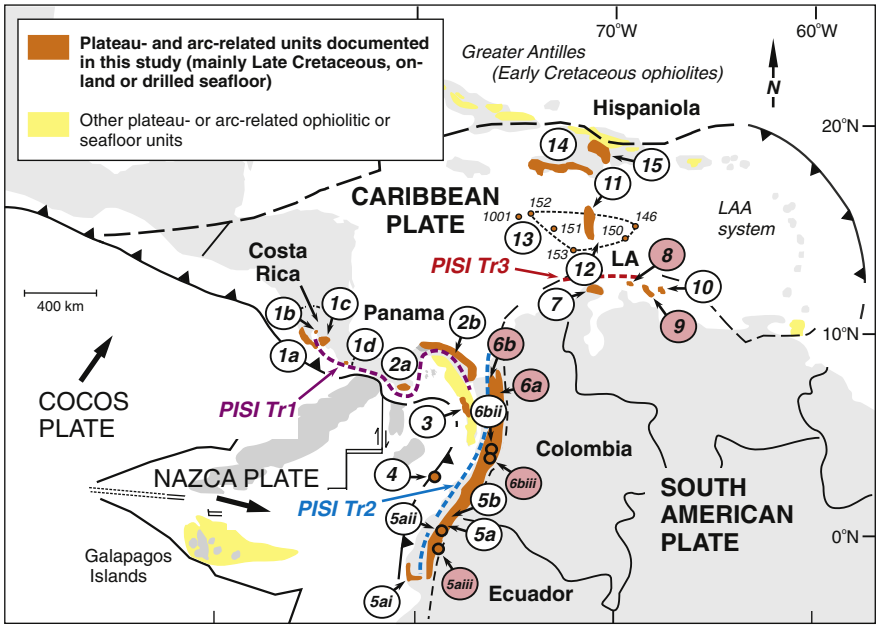

Plateau- and arc-related units

1a Nicoya Complex,
"old plateau", 140-110 Ma (OP)
"young plateau", 98-82 Ma (OP)
1b Tortugal Complex, 91-88 Ma (OP)
1c Herradura Complex, 88-82 Ma (OP)
1d Golfito Complex
1di Azuero Plateau ?, 89-85 Ma (OP)
1dii Golfito Arc, 75-66 Ma (PA)
2a Azuero Complex,
2ai Azuero Plateau, 89-85 Ma, (OP)
2aii Sona-Azuero Arc 73-69 Ma (PA, A)
2b Chagres-Bayano Arc, 70-39 Ma (A)
3 Serranía de Baudó Complex, 79-72 Ma (OP)
4 Gorgona Island, 91-81 Ma[a] (OP)
5a Pallatanga Unit, 90-85 Ma (OP)[b]
5ai Piñon Formation, 90-85 Ma (OP)
5aii Totoras Amphibolite, 87-82 Ma (meta OP[c])
5aiii Pujilí Granite, 87-81 Ma (A)
5b Rio Cala arc, ~85-64 Ma[d] (A)
6a Central Cordillera, 97-86 Ma, (OP)
6ai Antioquia Batholith, 95-86 Ma (A)
6b Western Cordillera, 94-75 Ma (OP) (***K***)
6bi Volcanic Formation[e] (101-98) (***V***)
6bii Bólivar UM Complex, 99-87 Ma (OP)
6biii Buga Batholith, 92-89 Ma (A)

7 Cabo de la Vela Complex ~83-65 Ma (A)
8 Aruba
8a Aruba Lava Formation,103-89 Ma[f] (OP)
8b Aruba Batholith, 90-79 Ma (A)
9 Curaçao
9a Curaçao Lava Formation, 120-62 Ma[g](OP)
9b Curaçao Diorite Intrusions, 87-85 Ma (A)
10 Bonaire, Albanian-Cenomanian (A, GAA)
11 Beata Ridge, 82-75 & 56-54 Ma (OP)
12 DSDP Leg 15, 97-87 Ma (OP)
13 ODP Leg 165, Site 1001, 82-80 Ma (OP)
14 Dumisseau Formation, Haiti, 98-82 Ma (OP)
15 Duarte Formation, Dominican Rep. 88-85 Ma (OP)

Plume-induced Subduction Initiation (PISI) traces

PISI Tr1, PISI trace 1
PISI Tr2, PISI trace 2
PISI Tr3, PISI trace 3

localities in which felsic, subduction-related, arc-like intrusive units temporally overlap the associated ~100-80 Ma oceanic plateau basement they intrude (see unit ages above and Fig. 2)

Fig. 1. Distribution of Cretaceous to Eocene Central American, NW South American and southern Caribbean (mostly post-100 Ma) plume- and arc-related (PAR) units. Also shown are the traces of the circa 100–90 Ma PISI event (dashed lines, see text in box). In the large box, unit names, locations are followed by age ranges (uncertainties rounded to the nearest Ma) and the current interpretation as oceanic plateau (OP), proto-arc (PA) or arc (A). Thick arrows represent present directions of plate movement. Superscripts (besides unit names or ages in box): *a*, age range of Kerr et al. (1996a) and Sinton et al. (1998), but we note that Serrano et al. (2011) record a much wider range in apparent ages of ~87–68 Ma; *b*, the Pallatanga Unit is considered to be correlative with other circa 90–85 Ma oceanic plateau units in western Ecuador including the Piñon Formation, and the Pedernale, Guaranda and related units (see Mamberti et al., 2003; Allibon et al., 2008); *c*, our interpretation is that the Totoras amphibolite represents the metamorphic sole of the 90–85 Ma western Ecuadorian oceanic plateau unit, see GR Online Supplementary Document; *d*, the oldest ages for the Rio Cala Arc will differ depending on whether one considers the La Portada Formation as part of the Rio Cala Arc or another system (see Kerr et al., 2002a and Vallejo et al., 2009); terminal magmatism at the Rio Cala Arc sensu stricto is likely about 72 Ma (Vallejo et al., 2009); *e*, the Volcanic Formation also includes the Barosso and Amaime formations (Villagómez et al., 2011) of the Western Cordillera (see Fig. 2); *f*, age range takes into consideration the circa 100 Ma radiometric age reported in Wright and Wyld (2011); *g*, controversy exists over the interpreted age range of the CLF (see Wright and Wyld, 2011); age incorporates the circa 115 Ma age reported in Wright and Wyld (2011). K and V in bold italics in brackets after *6b*, Western Cordillera and *6bi*, Volcanic Formation indicates that these references are from Kerr et al. (1997) and Villagómez et al. (2011), respectively. Complete references for all units shown are provided in Table 2. Abbreviations (on map): LA, Leeward Antilles; LAA, Lower Antilles Arc.

and 2; references in Table 2). Data are from (as numbered in Figs. 1 and 2): (*1a*) the Nicoya, (*1b*) Tortugal, (*1c*) Herradura and (*1d*) Golfito complexes, Costa Rica; (*2a*) the Azuero Complex which comprises the (*2ai*) Azuero Plateau and the (*2aii*) Sona–Azuero Arc; and (*2b*) the Chagres–Bayano Arc, Panama; (*3*) the Serranía de Baudó Complex, westernmost Colombia; (*4*) Gorgona Island, off of western Colombia; (*5a*) the Pallatanga and (*5ai*) Piñon Units and related oceanic plateau basement units and (*5b*) the Rio Cala and Macuchi arcs, western Ecuador; the (*6a*) Central Cordillera, (*6b*, *6bi*) Western Cordillera and (*6bii*) Bólivar Ultramafic Complex, western Colombia; the (*7*) Cabo de la Vela ultramafic–mafic Complex, northernmost Colombia (Guajira Peninsula); (*8a*) Aruba Lava Formation and (*9a*) Curaçao Lava Formation, Leeward Antilles; (*11*) the Beata Ridge, (*12*) DSDP Leg 15 and (*13*) ODP Leg 165, Site 1001, Caribbean Sea LIP basalts; and (*14*) the Dumisseau Formation, Haiti and (*15*) Lower Duarte Formation, Dominican Republic. In addition, we also compiled data for felsic, arc-related units which intrude or are spatially associated with plateau units in western Ecuador (*5aiii*, Pujili Granite), western Colombia (*6ai*,

Table 2
Summary of geologic units, tectonic setting, age and references.

Unit/complex No. (fr. Fig. 1)	Complex/unit	Region	Interpretation (OP, PA, or A)	Age (Ma)	References
PISI Tr1					
1a-old	Nicoya Complex	w. CR	OP	140–130, 110	Hoernle et al. (2004)
1a-young	Nicoya Complex	w. CR	OP	98–82	Sinton et al. (1997); Hauff et al. (2000a);
1b	Tortugal Complex	w. CR	OP	91–88	Alvarado et al. (1997); Hauff et al. (2000a)
1c	Herradura Complex	w. CR	OP	88–82	Sinton et al. (1997), Hauff et al. (2000a)
1d	Golfito Complex	w. CR	OP	Assumed to be ~80	Hauff et al. (2000a)
1d	Golfito Complex	s. CR	PA/A	*Maastrichtian* (*75–66*)	DiMarco et al. (1995); Buchs et al. (2010)
2a	Azuero Complex	s. PAN			
2ai	Azuero Plateau		OP	*Coniachian–early Santonian* (*89–85*)	Kolarsky et al. (1995); Buchs et al. (2009), Buchs et al. (2010); Wörner et al. (2009); Wegner et al. (2011)
2aii	Azuero Arc		PA, A	73–69	Wörner et al. (2009), Buchs et al. (2010), Wegner et al. (2011)
2b	Chagres–Bayano Arc	e. PAN	A	70–39	Wörner et al. (2009), Wegner et al. (2011), Montes et al. (2012)
PISI Tr2					
3	Serranía de Baudó Complex	w. COL	OP	79–72	Kerr et al. (1997)
4	Gorgona Island	w. COL	OP	91–81	Kerr et al. (1996a), Arndt et al. (1997), Walker et al. (1999); Révillon et al. (2000a)
4	Gorgona Island			101–59	Serrano et al. (2011)
5a	Pallatanga Unit	w. ECU	OP	90–85	Hughes and Bermúdez (1997), Boland et al. (2000), Kerr et al. (2002a), Hughes and Pilatsig (2002), Mamberti et al. (2003), Vallejo et al. (2009)
5ai	Piñon Formation			Turonian, 90–86	Jaillard et al. (1995, 2009), Luzieux et al. (2006)
5aii	Tortoras Amphibolite	w. ECU	meta. OP	87–82	Beaudon et al. (2005), Vallejo et al. (2006)
5aiii	Pujilí Granite	w. ECU	A	87–81	Spikings et al. (2005), Vallejo et al. (2006, 2009)
NA	San Juan	w. ECU	OP	136–110	Lapierre et al. (2000)
NA	San Juan	w. ECU	OP	101–98	Mamberti et al. (2004)
5b	Rio Cala Arc	w. ECU	A	85–64	Hughes and Bermúdez, 1997, Hughes and Pilatsig (2002); Kerr et al. (2002a), Vallejo et al.(2006, 2009), Chiaradia (2009), see also Boland et al. (2000)
NA	Macuchi Arc	w. ECU	A	44–33	Kerr et al., 2002a, Vallejo et al. (2009 and refs. therein), Chiaradia (2009)
6a	Central Cordillera	w. COL	OP	97–86	Kerr et al. (1997, 2002b)
6ai	Antioquia Batholith	w. COL	A	95–86	Villagómez et al. (2011)
6b	Western Cordillera	w. COL	OP	*Cenomanian–Conachian* (*97–87*), *94–75*	Barrero (1979), Bourgois et al. (1987), Kerr et al. (1997), see also Sinton et al. (1998) and Kerr et al. (2002b)
6bi	Volcanic, Amaime, & Barroso Fms. (of WC)	w.COL	OP	101–98	Villagómez et al. (2011)
6bii	Bólivar UM Complex (WC)	w. COL	OP	99–87	Kerr et al. (2004), Serrano et al. (2011), Villagómez et al. (2011)
6biii	Buga Batholith (WC)		A	92–89	Villagómez et al. (2011)
PISI Tr3					
7	Cabo de la Vela MUMC	n. COL/LA	A	83–65	Weber et al. (2009)
8	Aruba	LA			
8a	Aruba Lava Fm. (ALF)		OP	Turonian, 94–89	MacDonald (1968), White et al. (1999), see also Wright and Wyld (2011)
8b	Aruba Batholith		A	90–82	White et al. (1999), van der Lelij et al. (2010), Wright and Wyld (2011)
9	Curaçao	LA			
9a	Curaçao Lava Fm. (CLF)		OP	mid-Albian (~110), 120–78	Wiedmann (1978), Kerr et al. (1996b), Sinton et al. (1998), Wright and Wyld (2011)
9a				94–62	Loewen et al. (2013)
9b	Curaçao Diorite Intrusives		A	87–85	Wright and Wyld (2011), see also Sinton et al. (1998)
10	Bonaire	LA	A (of the GAA)	NA (as comprises GAA)	see Wright and Wyld (2011)
Center of Caribbean Plate					
11	CLIP, Leg 15	Carib. Sea	OP	97–87	Sinton et al. (1998)
12	Beata Ridge	Carib. Sea	OP	82–75, 56–54	Sinton et al. (1998), Révillon et al. (2000b), (see also Donnelly et al., 1973)
13	CLIP, Site 1001	Carib. Sea	OP	82–80	Sinton et al. (2000), Kerr et al.(2009)
Northern Caribbean Plate					
14	Dumisseau Formation	Haiti	OP	110–82	Sen et al. (1988), Sinton et al. (1998), Loewen et al. (2013)
15	Lower Duarte Formation	Dom. Rep.	OP	88–85	Lapierre et al. (1997, 1999)

This table. References for datasets of Caribbean plume- and arc-related units used in this study. The datasets include mostly age and geochemical data.
Footnotes:
Note that all radiometric ages listed here and elsewhere in the text encompass calculated ages plus and minor their uncertainties rounded to the nearest Ma, unless stated otherwise (e.g., as in Fig. 3). Radiometric ages are determined by $^{40}Ar/^{39}Ar$ or U–Pb zircon; all $^{40}Ar/^{39}Ar$ ages listed are plateau ages except those of the older Nicoya Complex (Hoernle et al., 2004) which are isochron (and agree within error of the uncertainties with the plateau ages). Plateau ages listed for the Curaçao and Dumisseau formations of the study of Loewen et al. (2013) include only those deemed as reliable plateau ages (by Loewen et al., 2013). Similarly, the age range for Gorgona of the study of Serrano et al. (2011) includes plateau ages only. The only K–Ar ages listed are those for the Cabo de la Vela Complex. Biochronologic ages are in italics. The radiometric age of 94–89 Ma for the ALF is based on a U–Pb age of 97.3 ± 8.2 Ma of an ALF gabbro as reported by Wright and Wyld (2011), whereas the Turonian age is based on ammonites intercalated with ALF basalts (MacDonald, 1968). Abbreviations: A, arc; COL, Colombia; CR, Costa Rica; ECU, Ecuador; GAA, Greater Antilles Arc; LA, Leeward Antilles; meta. OP, metamorphosed OP; MUMC, mafic-ultramafic complex OP, oceanic plateau; PA, proto-arc; PAN, Panama; OP; WC, Western Cordillera (of western Colombia).

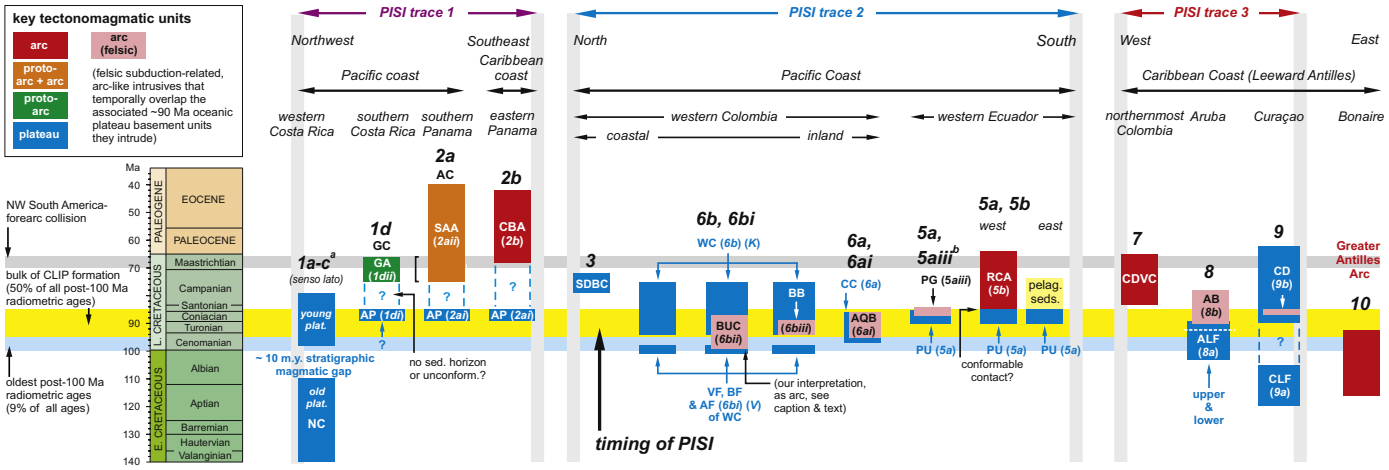

Fig. 2. Simplified stratigraphic relations of Cretaceous to Eocene Central American, NW South American and southern Caribbean plume- and arc-related (PAR) units from this study to demonstrate relations between underlying units interpreted as plateau and overlying ones interpreted as arc. Units numbered as in Fig. 1. The bulk of CLIP formation appears to have occurred at 95–85 Ma (thick, yellow, horizontal line, see Fig. 3). We infer that the time of plume-induced subduction initiation (PISI) began during this time (~95–85 Ma). The collective data suggests that the SI event is traceable along southern Central America (PISI trace 1, Costa Rica and Panama); northwestern south America (PISI trace 2, western Ecuador and western Colombia); and in the southern Caribbean in the Leeward Antilles (PISI trace 3, Aruba and Curacao). References and ages for PAR units are in Table 2 and the majority of stratigraphic relations are 'constructed' on the basis of these ages; exceptions include the stratigraphic columns for *1d* and *2a* which are from Buchs et al. (2010) and the stratigraphic columns for *5a*, *b* which are from Vallejo et al. (2009). Unit acronyms: AC, Azuero Complex; ALF, Aruba Lava Formation; AF, Anime Formation; AP, Azuero Platteau; AQB, Antioquia Batholith; BB, Buga Batholith; BF, Barosso Formation; BUC, Bólivar Ultramafic Complex; CBA, Chagres–Bayano Arc; CC, Central Cordillera; CD, Curaçao Diorites; CDVC, Cabo de la Vela Complex; CLF, Curacao Lava Formation; GA, Golfito Arc; NC, Nicoya Complex; PG, Pujilí Granite; PU, Pallatanga Unit; RCA, Rio Cala Arc; SDBC, Serranía de Baudó Complex; VF, Volcanic Formation; WC, Western Cordillera. K and V in bold italics in brackets after *6b*, Western Cordillera and *6bi*, Volcanic Formation indicates that these references are from Kerr et al. (1997) and Villagómez et al. (2011), respectively. Superscripts, main figure: *a*, represents the age range for the Nicoya, Tortugal and Herradura complexes, which might represent separate units (see Bandini et al., 2008; Baumgartner et al., 2008) and not the Nicoya Complex sensu stricto; *b* (beside *5aiii*), the (original) stratigraphic relation between the Pujilí granite and Pallatanga Unit are uncertain, hence the question mark (see Vallejo et al., 2006).

Antioquia and *6bii*, Buga batholiths), Aruba (*8b*, Aruba Batholith) and Curaçao (*9b*, Curaçao diorites). These compilations include data for ~400 samples. Datasets for *11-15* are of igneous rocks removed from subduction-affected regions along the three PISI traces and thus provide useful baseline information about the plume mantle source, unaffected by subduction inputs, against which data for PAR sequences can be compared. Further details about samples and methods of data manipulation are provided in the GR Online Supplementary Document.

3.2. Compilations of basalt geochemistry from other relevant tectonic environments

To better illuminate the tectonic environments where Late Cretaceous Caribbean PAR sequences formed, we also compiled geochemical data for lavas from representative examples of three distinct tectonomagmatic associations: (1) oceanic plateau basalts (OPB); (2) volcanic arc basalts (VAB); and (3) basalts erupted during subduction initiation. The OPB dataset ($n = 353$) compiles tholeiitic basalts from four OP in the Pacific Ocean: Ontong Java (Mahoney et al., 1993; Tejada et al., 2002), Manihiki (Hoernle et al., 2010) and Hikurangi (Hoernle et al., 2010) plateaus and the Shatsky Rise (Sano et al., 2012); and the Kerguelen Plateau (Mahoney et al., 1995; Frey et al., 2002; Neal et al., 2002), Indian Ocean. Although many more datasets exist for global OPB the compilation of nearly 400 OPB samples we have amassed is more than adequate to serve for comparison with Caribbean OPB. The volcanic arc basalt (VAB) datasets comprise Quaternary lavas from the Central American and Izu-Bonin Mariana (IBM) arc (as compiled by Jordan et al., 2012). The Central American Arc dataset comprises lavas (arc basalts, $n = 1052$) from Quaternary volcanoes in Costa Rica, Nicaragua, El Salvador and Guatemala. Izu-Bonin Marianas forearc basalts (Reagan et al., 2010) formed at the beginning of subduction beneath this arc. Data compiled for ophiolites that follow the 'subduction initiation rule' of Whattam and Stern (2011) includes lower and upper ophiolite unit basalts and basaltic andesites that comprise the Pindos, Mirdita, Troodos and Semail ophiolites (as compiled by Whattam and Stern, 2011). The subduction initiation rule ophiolite basalts and IBM forearc basalts ($n = 29$) are interpreted to have formed in a similar manner during SI (Whattam and Stern, 2011; Reagan et al., 2013). Additionally, we also use compositions of mid-oceanic ridge basalts (MORB) and oceanic island basalts (OIB) (Sun and McDonough, 1989) and bulk continental crust (BCC) (Rudnick & Gao, 2003) for further comparison.

3.3. Age data

We compiled 100 radiometric dates (5 Ma bins) in addition to biostratigraphic age determinations of samples from units interpreted as CLIP and present these in Fig. 3. We used this database to assign ages to each PAR unit so that geochemical characteristics are securely placed in a temporal framework.

4. Results

Compiled geochemical and geochronological datasets allow us to demonstrate two main features that – in conjunction with stratigraphic relations and tectonic considerations – are consistent with a PISI model (see Section 5) for southern Central American and NW South American plume- and arc-related complexes: (1) the chemistry of most post-100 Ma units along Central America and NW South America interpreted as CLIP show a progressive evolution to higher degrees of partial melting and increasing subduction additions with time beginning at 100 Ma; and (2) the rapid transformation from plateau to arc environment beginning ~100 Ma.

4.1. Age of the CLIP and the timing of inception of arc igneous activity

The summary of age information (Fig. 3) reveals two salient features: (1) the existence of two phases of plateau construction before and after 100 Ma; and (2) a main pulse of magmatic activity between 95 and 85 Ma. The first phase between 140 and 110 Ma appears to be volumetrically subordinate as it comprises only 8% of all radiometric dates but it remains uncertain as to the actual volumetric percentage

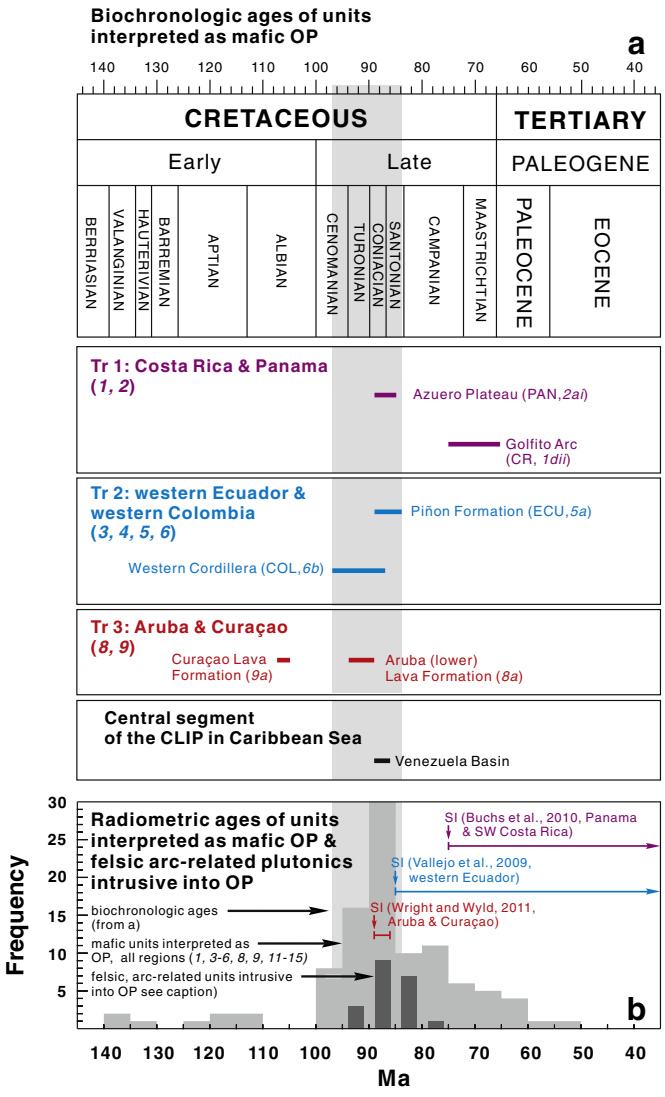

Fig. 3. Distribution and frequency of (a) biostratigraphic and (b) radiometric age determinations of plateau- and arc-related units of this study along traces 1, 2 and 3 (Tr1, Tr2, Tr3) and the central segment of the Caribbean Sea. Radiometric dates are binned on the basis of calculated ages without consideration of uncertainties. The gray bar in (a) is for visual aid to underscore that most biochronologic age determinations correlate with the highest frequency of radiometric age determinations (at ~95–85 Ma, as shown in (b)). The distribution and frequency of radiometric age determinations subdivided on the basis of region and individual units are provided in Figs. A1 and A2, respectively, of the GR Online Supplementary Document. References for the age of units plotted are provided in Table 2 apart from the Venezuelan Basin age data which is from Donnelly et al. (1973). The numbers in italics in brackets beside the region or unit name corresponds to the unit numbers assigned in Fig. 1.

of older vs. younger basalts because more older lavas must be buried under younger lavas. These older ages come from the western and southeastern limits of the study area. In the west, these ages are from the Nicoya Complex, Costa Rica (five of eight pre-100 Ma ages) (Hoernle et al., 2004). In the southeast, these ages are found in the San Juan oceanic plateau unit, western Ecuador dated as 123 ± 13 Ma via Sm–Nd isochron (Lapierre et al., 2000). In the northeast, early plume activity is documented for the 97.3 ± 5.2 Ma lower Aruba Formation and 112.7 ± 7.3 Ma Curacao Lava Formation (see Wright and Wyld, 2011).

Although it is not possible to evaluate the extent to which age distributions may be biased, we note that the radiometric and biostratigraphic ages agree reasonably well (Fig. 3). We do not know how representative the number of ages is of the volumes of CLIP magmas through time, but Fig. 3 nonetheless demonstrates a steady climb in the frequency of ages between 100 and 95 Ma ($n = 8$), 95–90 Ma ($n = 16$) and 90–85 Ma ($n = 30$) followed by decreasing frequency thereafter. We interpret this to indicate that the major pulse of CLIP magmatic activity occurred between 95 and 85 Ma (46% of all radiometric age determinations of mafic rocks interpreted as CLIP) and that CLIP magmatic activity subsequently waned.

Our age compilation (Fig. 3) is broadly consistent with earlier studies concluding that CLIP plume activity mainly occurred between 92 and 88 Ma with minor magmatic pulses at 124–112 Ma and 76–72 Ma (Sinton et al., 1998; Kerr et al., 2003). A more recent study (Serrano et al., 2011) concludes that CLIP plume activity continued uninterrupted until the end of the Cretaceous. Ages younger than ~80 Ma however are mostly from the middle of the Caribbean Sea and Curaçao in the Leeward Antilles. Most post-80 Ma ages elsewhere are confined to Gorgona Island off western Colombia (Serrano et al., 2011) and the Serranía de Baudó unit (Kerr et al., 1997) of western Colombia (see Supplementary Figs. 1 and 2 which split the radiometric ages into regions and discrete units). In the case of the Gorgona Complex, earlier studies (Kerr et al., 1996a and studies cited therein) yield ages of 91–81 Ma; only three samples from the dataset of Serrano et al. (2011) yield reliable younger circa 75–70 Ma ages which is similar to the age of terminal magmatism in the Serranía de Baudó Complex (~72 Ma, Kerr et al., 1997). Moreover, there has been disagreement as to which units represent plateau and which represent arc. For example, Hauff et al. (2000a,b) considered the 75–66 Ma Golfito Complex of southern Costa Rica to be a plateau sequence, whereas Buchs et al. (2010) reinterpreted this as arc. Thus, if the former interpretation is held, 'plateau' magmatism extended until 66 Ma but only until ~80 Ma if the latter interpretation is considered. Similarly, and as we develop in Section 4.2, both the Serranía de Baudó and Gorgona units interpreted as plateau record obvious subduction-derived modifications and termination of magmatism at 75–70 Ma is consistent with the timing of termination of subduction-related magmatism elsewhere along the western margin of NW South America. For example, the cessation of magmatism at Gorgona and Serranía de Baudó coincides with the termination of arc magmatism to the north (Cabo de la Vela Complex by ~74 Ma, Weber et al., 2009) and to the south (Rio Cala Arc, western Ecuador by ~72 Ma, Vallejo et al., 2009) and is coincident with South America-forearc collision at 73–70 Ma (Vallejo et al., 2009) and the emplacement of subduction-modified plateau units upon western South America soon thereafter.

CLIP plume activity mainly occurred between 95 and 85 Ma (Fig. 3) and may have effectively buried Early Cretaceous oceanic crust. Younger CLIP ages are essentially confined to the center of the CLIP (e.g., Beata Ridge, terminal magmatism at ~54 Ma (Révillon et al., 2000b)) and the Leeward Antilles (e.g., Curaçao, terminal magmatism at ~62 Ma, (Loewen et al., 2013)).

Our goal is to understand how the CLIP and the three 1000-km long PISI traces evolved to the modern arc that now occupies Central America and Ecuador–Colombia. We assume that subduction of various Pacific oceanic plates (Farallon, Cocos, Nazca) beneath Tr1 and Tr2 has been continuous since east-dipping subduction began in the Late Cretaceous. The first step to understanding what happened is to reconstruct when it happened. Plume activity was especially intense at 95–85 Ma and arc volcanism in Tr1 began by at least 75 Ma (Buchs et al., 2010) and in Tr2 by 85 Ma (Vallejo et al., 2009). Independent constraints on the minimum age of subduction are 60 Ma based on the oldest accreted Galapagos hotspot tracks (Hoernle et al., 2002). Arc igneous activity and therefore subduction was very brief along Tr3 in the Leeward Antilles but left distinctive calc-alkaline intrusive suites in Aruba and Curacao (Aruba Batholith, ~92–78 Ma, White et al., 1999; van der Lelij et al., 2010; Wright and Wyld, 2011; Curacao Diorites, ~82–80 Ma, Wright and Wyld, 2011) which indicates that subduction took place 89–86 Ma along Tr3 (Wright and Wyld, 2011). These ages are broadly consistent with results from studies of the Villa de Cura belt of northern Venezuela, where blueschist facies metamorphism is interpreted to

Table 3
Summary of geologic units, age, and diagnostic chemical features.

Unit/ complex	Complex/unit	Age	Region	Interpretation	THI	*n*	Ti/V			Partial melting proxy Nb/Yb			Subduction proxy Ba/Th			Ba/Nb			Th/Nb		
No. (fr. Fig. 1)		(Ma)		(OP, PA, or A)	mean	TNSS: Fe4.0, Fe8.0	mean	range	*n*	mean	range	*n*	mean	range	*n*	mean	range	*n*	mean	range	*n*
PISI Tr1																					
1a-old	Nicoya Complex	140–130, 110	w. CR	OP	NC				1	1.82	1.65–2.07	5	87.12	73.42–118.73	5	5.97	4.88–8.39	5	0.07	0.07–0.07	5
1a-young	Nicoya Complex	98–82	w. CR	OP	1.50	49: 3, 31	21.20	16.90–27.63	42	1.72	1.36–2.38	30	201.78	27.27–1414.81	30	11.94	1.97–92.49	30	0.06	0.04–0.08	30
1b	Tortugal Complex[a]	91–88	w. CR	OP																	
	depleted basalt (BC-17)		w. CR	OP			19.26		1	1.34		1	100		1	7.28		1	0.07		1
	enriched basalt (BC-18)		w. CR	OP			18.57		1	10.3		1	88.69		1	6.43		1	0.07		1
	BC-16 (relative 'depletedness' unknown)						60.00														
1c	Herradura Complex	88–82	w. CR	OP	NC		22.54	17.83–40.62	8	1.63	1.41–1.96	4	132.41	116.67–153.33	4	8.58	7.07–9.62	4	0.06	0.06–0.07	4
1d(H)	Golfito Complex	assumed to be ~80	w. CR	OP	1.15	4: 1, 1	22.31	17.74–25.45	4	1.25	1.06–1.63	3	208.55	82.61–355.56	3	21.14	5.29–32.43	3	0.10	0.06–0.14	3
1d(B)	Golfito Complex	*Maastrichtian (75–66)*	s. CR	PA/A	1.21	8: 1, 3	18.02	14.64–21.32	4	0.95	0.68–1.20	4	644.28	400.00–877.27	3	63.22	51.10–85.02	4	0.10	0.08–0.13	3
2a	Azuero Complex		s. PAN																		
	Azuero Plateau	*Coniacian-early Santonian 89–85*		OP																	
	depleted basalts				0.97[A]	33: 1, 29	22.20	17.05–38.86	32	1.43	0.70–1.77	32	202.94	39.13–1350.00	32	14.44	2.70–95.86	32	0.07	0.06–0.22	32
	enriched basalts				NA		40.00	38.92–41.07		4.76	4.31–5.22	2	242.44	51.96–432.93	2	15.89	3.30–28.49	2	0.06	0.06–0.07	2
2ai	Azuero Arc	73–69		PA, A	0.77	38: 13, 4	24.69	14.62–33.04	14	1.41	0.65–2.66	14	292.34	623.81–4092.71	14	32.47	9.11–63.60	14	0.13	0.08–0.46	14
2b	Chagres-Bayano Arc	70–39	e. PAN	A	1.02	73: 20, 10	15.25	5.69–24.47	24	0.68	0.17–4.21	23	806.54	65.22–6657.14	24	287.18	15.31–1696.82	23	0.43	0.09–1.74	23
PISI Tr2																					
3	Serranía de Baudó Complex	79–72	w. COL	OP																	
	depleted basalts				NC		23.18	15.72–23.18	18	1.35	0.92–1.96	6	118.96	83.87–225.00	6	22.54	4.29–75.38	18	0.12	0.07–0.24	6
	enriched basalts				0.66	3: 1, 2	47.64	45.08–48.94	3	5.69		1	875.63		1	36.92	6.58–70.41	3	0.08		1
4	Gorgona Island depleted	91–81	w. COL	OP																	
	bas				NC		15.72		1	0.66	0.55–0.78	3	339.24	121.82–556.67	2	10.76	9.38–12.10	3	0.06	0.02–0.09	2
	pics				NC		11.71	10.65–12.96	6	0.22	0.16–0.34	4	225.28	60.00–313.33	3	23.40	7.20–40.87	4	0.11	0.09–0.13	3
	koms				NC		16.23	11.94–23.68	14	0.40	0.29–0.54	9	2231.75	85.33–7885.00	4	86.82	4.91–358.41	9	0.12	0.05–0.31	4
	enriched basalts				NC		30.70	17.08–41.24	3	8.07	4.42–11.24	4	74.94		1	3.36	1.68–5.00	4	0.06		1
4(S)	Gorgona Island	101–59																			
	depleted bas[b]	*69–59*			NC		17.42		1	1.82		1	245.46		1	14.48		1	0.06		1
	depleted koms	assumed to be Late Cretaceous			NC		15.54	14.87–16.22	2	0.28	0.28–0.29	2	154.39	106.55–202.23	2	10.42	7.22–13.62	2	0.07	0.07–0.07	2
	enriched koms	*87–84*			NC		10.82		1	5.34		1	55.24		1	3.81		1	0.07		1
	enriched basalts	*71–68*			NC		18.56		1	1.93		1	44.92		1	2.83		1	0.06		1
	gabbro	*101–96*			NC		15.58			1.53		1	143.14		1	8.36		1	0.06		1
5a	Pallatanga Unit & others[c]	90–85	w. ECU	OP																	
	basalts[d]				NC		21.65	16.51–28.14	34	1.65	0.75–1.92	27	279.20	19.00–2475.38	34	16.99	1.82–136.94	31	0.08	0.04–0.25	32
	picrites				NC		17.67	16.58–19.09	4	0.92	0.75–1.36	4	232.52	140.75–398.00	4	9.81	6.70–13.23	4	0.04	0.03–0.05	4
	ankaramites				NC		21.86	18.85–26.10	6	3.58	1.80–6.42	5	256.93	31.52–604.55	6	14.08	1.74–41.30	6	0.07	0.05	6
5b	Rio Cala Arc	85–64	w. ECU	A	1.16	12: 3, 4	14.66	13.55–15.80	3	1.92	0.29–2.51	8	201.98	103.33–247.60	8	147.91	34.44–222.06	8	0.70	0.33–0.90	8
NA	Macuchi Arc	44–33	w. ECU	A	NC		17.63	14.87–20.07	3	0.61	0.44–0.86	3	288.31	78.05–605.26	3	183.75	32.99–466.22	3	0.49	0.29–0.77	3
6a	Central Cordillera	97–86	w. COL	OP																	
	basalts				1.49	23: 1, 11	20.39	7.70–36.91	22	2.68	0.54–7.24	4	78.01	60.47–104.65	3	8.03	0.73–21.43	21	0.09	0.08–0.10	3
	picrites				NC		34.29	15.97–80.72	17	6.66	1.55–19.52	15	224.38	36.84–603.64	4	15.55	2.79–59.52	17	0.15	0.04–0.41	4
6b	Western Cordillera	94–75	w. COL	OP	NC		22.61	18.44–36.43	26	1.49	0.77–1.89	12	399.98	43.55–1380.00	9	40.70	6.28–172.50	12	0.08	0.07–0.10	9
6bi	Volcanic, Amaime, & Barroso Fms. (of the Western	101–98	w.COL	OP			18.74	14.72–22.72	9	1.69	1.24–2.71	9	513.88	48–1975	9	37.14	4.02–158.84	9	0.07	0.05–0.10	9

(continued on next page)

Table 3 *(continued)*

Unit/ complex	Complex/unit	Age	Region	Interpretation	THI	*n*	Ti/V			Partial melting proxy Nb/Yb			Subduction proxy Ba/Th			Ba/Nb			Th/Nb		
No. (fr. Fig. 1)		(Ma)		(OP, PA, or A)	mean	TNSS: Fe4.0, Fe8.0	mean	range	*n*	mean	range	*n*	mean	range	*n*	mean	range	*n*	mean	range	*n*
	Cordillera)																				
6bii	Bólivar UM Complex (WC) basalt	99–87	w. COL	OP	NA		22.76		1	1.68		1	47.45		1	3.26		1	0.07		1
PISI Tr3																					
7	Cabo de la Vela MUMC	83–65	n. COL/LA	A																	
	lower gabbros (basaltic–andesites)						12.51	11.70–13.32	2												
	lastest stage dykes (basaltic–andesites)				1.69[B]	4: 2, 1	17.27	13.72–20.81	2	0.43	0.26–0.60	2	571.50	461.50–681.50	2	485.60	426.00–545.20	2	0.86	0.80–0.92	2
8	Aruba		LA																		
8a	Aruba Lava Fm. (ALF)	*Turonian*, 94–89		OP	NC					1.95	1.76–2.15	7	156.43	83.78–332.43	7	11.48	6.74–26.74	7	0.07	0.07–0.08	7
9	Curaçao		LA																		
9a	Curaçao Lava Fm. (CLF)	*mid-Albian (~110)*, 120–78		OP																	
	basalts				NC		18.65	17.29–24.50	14	2.09	1.73–2.60	12	73.04	28.55–111.05	3	9.43	1.94–59.68	14	0.06	0.05–0.07	3
	picrites				NC		20.76	17.67–26.85	12	2.67	2.13–5.00	8	93.19	19.92–204.42	4	7.16	1.26–13.86	12	0.08	0.06–0.10	4
	basalt	*78–74*			NC		22.62		1	2.19		1	45.38		1	1.97		1	0.04		1
9a (L)[R]		94–62																			
	basalt	*93–92*			NC		17.69		1	1.99		1	107.38			8.13		1	0.08		
	basalt	*77–72*			NC		19.96		1	1.83		1	88.96		1	5.81		1	0.07		1
	basalts	*64–62*			NC		19.32	18.93–19.71	2	1.56	1.40–1.72	2	65.90	47.87–83.94		6.13	3.33–8.94	2	0.09	0.07–0.11	2
Center of Caribbean Plate																					
11	CLIP, Leg 15	97–87	Carib. Sea	OP																	
	basalts				NC					1.41	0.49–1.81	10	44.41	33.33–49.58	10	3.21	2.44–3.74	10	0.07	0.06–0.08	10
	enriched basalts				NC					9.62	9.22–10.02	2	25.48	25.00–25.96	2	2.06	1.99–2.13	2	0.08	0.08–0.08	2
12[R]	Beata Ridge	82–75, 56–54	Carib. Sea	OP																	
	depleted dolerites	82–78, 56–54					23.47	23.22–23.73		1.53	1.16–1.89	2	66.03	47.70–84.37	2	5.81	5.21–6.40	2	0.09	0.08–0.11	2
	enriched basalts	79–75					70.91			43.06		1	115.33		1	2.85		1	0.02		1
	dolerites (relative 'depletedness' unknown)	79–78					30.31	21.33–39.30				2			2	22.23	12.92–31.54	2			2
13	CLIP, Site 1001 basalts	82–80	Carib. Sea	OP	NC		22.77	20.62–25.64	14	0.47	0.36–0.57	14	161.24	60–921.43	14	8.41	2.93–52.02	14	0.05	0.04–0.06	14
Northern Caribbean Plate																					
14[R]	Dumisseau Formation	110–82	Haiti	OP																	
		110–100			NA		21.19		1	1.04		1	60.00		1	6.07		1	0.10		1
		96–82			1.07	12: 1, 2	46.44	38.65–53.12	12	5.19	4.54–5.93	12	50.44	33.33–62.96	12	3.69	2.39–4.56	12	0.07	0.07–0.08	12
15[R]	Lower Duarte Formation	*88–85*	Dom. Rep.	OP						6.93	4.69–9.18	2							0.06	0.06–0.07	2

Tectono-magmatic suite	THI	*n*	Ti/V			Nb/Yb			Ba/Th			Ba/Nb			Th/Nb		
	mean	TNSS: Fe4.0, Fe8.0	mean	range	*n*	mean	range	*n*	mean	range	*n*	mean	range	*n*	mean	range	*n*
OPB	1.21	353: 7, 152	27.96	17.40–50.51	351	2.33	0.24–11.45	287	77.75	23.21–621.88	27	5.52	2.0–38.0	27	0.08	0.03–0.13	299
OIB	NC		75.00			22.22			87.50			7.29			0.08		
N-MORB	NC		35.00			0.76			52.50			2.70			0.05		
SIRO lower	0.96	58: 10, 13	29.51	12.20–48.43	34	0.51	0.18–1.38	12	50.05	8.11–188.89	12	5.05	0.55–22.67	14	0.10	0.06–0.15	12
IBMFAB	1.04	18: 1, 9	15.22	12.03–18.45	12	0.52	0.35–0.70	12	89.28	20.77–337.50	12	7.15	2.89–23.28	12	0.09	0.07–0.19	12
SIRO upper	1.03	66: 16, 12	13.44	8.50–23.71	11	0.39	0.13–0.93	9	230.03	75.00–418.52	8	53.93	17.39–87.72	9	0.26	0.11–0.32	8
CAVA	0.83	583: 287, 50	21.32	9.99–57.80	146	2.48	0.38–12.21	97	600.46	37.04–2085.85	101	191.58	2.33–750.91	110	0.37	0.03–1.44	91
IBMVA	1.19	1436: 836, 24	16.37	8.45–21.96	138	0.37	0.10–3.38	138	478.48	26.79–1110.42	163	168.70	49.00–1023.53	195	0.55	0.12–2.33	137

have accompanied the initiation of subduction at 96.3 ± 0.4 Ma (Smith et al., 1999).

4.2. Changes in magma composition at and after arc inception

We cannot yet resolve all of the details of how the three subduction zones (i.e., along Tr1, Tr2, Tr3) formed and whether or not these three zones formed in a single event and shared a common early history. Nevertheless, a record of how their mantle sources evolved is available in the geochemistry of their lavas coupled with geochronological constraints. Below, we use geochronologically-constrained chemical compositions to probe the mantle source of PAR melts to elucidate how the following tectonically-sensitive characteristics changed with time: (1) Tholeiitic vs. calc-alkaline magmatic differentiation as resolved by SiO_2 vs. FeO^t/MgO and $Na_2O + K_2O$–FeO^t/MgO (AFM) relations and tholeiitic index (THI, Section 4.2.1). Differentiation of subalkaline igneous suites following the distinctive calc-alkaline trend of no iron enrichment as silica increases reveal a clear supra-subduction zone (SSZ) tectonic environment. These differences largely reflect the much higher magmatic water contents in arc magmas. (2) Mantle source depletion and relative degrees of partial melting that generated these melts, as gauged by Nb/Yb (Section 4.2.2). Arc magmas are generated by melting mantle that is much more depleted than that which generates MORB and OIB. (3) Oxygen fugacity of the mantle source as monitored by Ti/V (Section 4.2.3). Peridotite xenoliths show that the oxygen fugacity of the uppermost mantle furthest away from subduction zones – for example that of mantle plumes – has oxygen fugacities equal to or 1–2 log units lower than the fayalite–magnetite–quartz (FMQ) oxygen buffer, whereas arc peridotite is more oxidized, up to 4 log units above FMQ (Frost and McCammon, 2008; Evans et al., 2012). If the source region received simultaneous plume and subduction contributions this may be reflected in variations of Ti/V ratios. Finally, (4) Relative contributions from the subducted slab as identified by subduction markers of Ba/Th, Ba/Nb and Th/Nb (Section 4.2.4). Progressive squeezing and heating of subducted oceanic crust and sediments firstly releases hydrous fluids which are followed by sediment melts. Trace elements such as Ba and Th are sensitive to such inputs. We carry out these geochemical interrogations below using the geochemical proxies outlined above. Table 3 provides the mean and range of these proxies (THI, Nb/Yb, Ti/V, and Ba/Th, Ba/Nb, Th/Nb) for unit lavas of this study; Table 3 also provides the means and ranges of these proxies for OPB, VAB, N-MORB, OIB and subduction initiation basalts (see Section 3.2) for comparison with plume- and arc-related units of this study.

Our PISI model (Section 5) predicts that SI occurred after 100 Ma due to lithospheric weakening accompanying the arrival of the volumetrically dominant post-100 Ma Caribbean mantle plume and that evidence of this SI event is preserved in PAR sequences along the three ~1000 km long traces: Tr1 in NW Costa Rica through Panama; Tr2 from western Ecuador through Colombia; and Tr3 through the westerly Leeward Antilles. PAR units in these three traces should have chemical compositions that are: (1) similar to each other and distinct from 'normal' OPB elsewhere; and (2) distinct from the pre-100 Ma unit (e.g., 140–110 Ma Nicoya Complex fragment) and post-100 Ma units in regions further north where subduction modification of the mantle plume is unlikely to have occurred (e.g., ODP drill sites in the middle of the Caribbean Plate, central Hispaniola in the northern segment of the CLIP). Our model thus further predicts that both the older Nicoya Complex and CLIP units drilled by ODP to be more like global OPB than post-100 Ma PAR units exposed along the three PISI traces.

Below, we test the PISI model using the aforementioned key geochemical proxies to highlight progressive post-100 Ma changes in the melting source of PAR units with time, including tholeiitic vs. calc-alkaline affinities (Section 4.2.1), partial melting and source fertility (Section 4.2.2), source oxygen fugacity (Section 4.2.3), and subduction component additions (Section 4.2.4). Constraints from alteration-resistant radiogenic isotopes (Nd and Pb) are summarized in Section 4.3.

4.2.1. Temporal variations of tholeiitic and calc-alkaline affinities

Magmatic differentiation trends with or without iron enrichment provide information about tectonic environment of formation. Igneous sequences with calc-alkaline affinities (no iron enrichment) are diagnostic of convergent margin suites whereas basalts from multiple tectonic environments (including convergent margins) show tholeiitic (iron enrichment) trends. Thus, arc units are sometimes tholeiitic but calc-alkaline suites are invariably subduction-related (Barbarin, 1999). We use SiO_2 vs. FeO^t/MgO (Miyahsiro, 1974; Arculus, 2003) and Na_2O–FeO^t–MgO (AFM, total alkalis–iron–magnesium) (Kuno, 1968; Irvine and Baragar, 1971) relations and the tholeiitic index (THI) (Zimmer et al., 2010) to discern tholeiitic vs. calc-alkaline affinities through time for plateau- and arc-related units of this study.

SiO_2 vs. FeO^t/MgO relations demonstrate that most lavas and intrusives of basaltic or sub-basaltic composition from units interpreted as CLIP overlap the tholeiitic–calc-alkaline subdivision of Miyashiro (1974) and plot as medium-Fe subalkaline series of Arculus (2003) (Fig. 4a). On the AFM plot (Fig. 4b) all Caribbean units display obvious Fe-enrichment trends (Fig. 4b) however, a minority of PAR basalts exposed along Tr1, Tr2 and Tr3 plot as calc-alkaline. Moreover, compositions of rocks along these traces evolve to calc-alkaline affinities with time and increasing differentiation (see also Fig. 12a which demonstrates the calc-alkaline affinity of Late Cretaceous felsic, arc-like units from western Ecuador and Colombia and the Leeward Antilles along Tr2 and Tr3). For example, whereas most of the circa 100–75 Ma Ecuadorian and Colombian samples plot within the medium-Fe series field, the 79–72 Ma Serranía de Baudó Complex (westernmost Colombia) plot almost entirely within the low-Fe (calc-alkaline) field (Fig. 4a, second plot from the top). It is noteworthy that the oldest units and those of the central and northernmost Caribbean Plate exhibit the strongest Fe-enrichment trends. The only units which have basalts/basaltic intrusives that display nearly vertical trends in SiO_2 vs. FeO^t/MgO space and which plot (almost) entirely within the high-Fe series are ones from the Nicoya Complex in Costa Rica and the Beata Ridge and Hispaniola, from the center and northernmost segments of the

Notes to Table 3:

This table. Tholeiitic index (THI), Nb/Yb, Ti/V, Ba/Th, Ba/Nb and Th/Nb of volcanic rocks of Caribbean plume- and arc-related units from this study which are plotted in Figs. 4–9. Also listed are these geochemical proxies of oceanic plateau basalts (OPB), oceanic island basalts (OIB), N-MORB, lower and upper units of subduction initiation rule ophiolites (SIRO lower, SIRO upper), Izu-Bonin Mariana forearc basalts (IBMFAB), the Central American Volcanic Arc (CAVA) and the Izu-Bonin Mariana Volcanic Arc (IBMVA) volcanic arc. References for the Caribbean units are provided in Table 2 and references for OPB, SIRO, IBMFAB, CAVA and IBMVA are listed in Section 3.2. Data for OIB and N-MORB are from Sun and McDonough (1989).

Footnotes:

Note that all radiometric ages listed here and elsewhere in the text encompass calculated ages plus and minus their uncertainties rounded to the nearest Ma, unless stated otherwise (e.g., as in Fig. 3). See Table 2 caption for other age details. Letters H, B, S, and L beside Unit/Complex numbers in column one are to denote that the data is from Hauff et al. (2000a), Buchs et al. (2010), Serrano et al. (2011) and Loewen et al. (2013). Superscript R, beside Unit/Complex numbers in column one is to denote that all samples of these units have corresponding radiometric ages. Superscripts beside unit names in the Complex/Unit (second) column: a, as all Tortugal alkali basalts and picrites have total oxides <97 wt.% and thus do not pass our total oxides filter of 97–102 wt.% (see GR Online Supplementary Document), ratios were not calculated for these; b, Serrano et al. (2011) interpret this 69–59 Ma basalt as an enriched basalt but its flat chondrite-normalized REE pattern suggests that is a depleted basalt; c, ratios presented include those for other basement considered as correlatives of the circa 90–85 Ma Pallantanga Unit including the Piñon, Pedernales and Guaranda units (see Mamberti et al., 2003); d, one Pallatanga Unit sample (97 Ma13, Mamberti et al., 2003) with anomalously high Ba (4779 ppm) has been omitted from our calculations as we assume this to be a typo, e.g., the remaining samples exhibit a mean of 57 ppm Ba with a range from 8 to 322 ppm Ba. Superscripts beside THI mean in THI column: A, as no Azuero depleted basalts have 3–5 wt.% MgO, calculation of THI was done with a single sample with 5.30 wt.% MgO; B, $Fe_{4.0}$ and $Fe_{8.0}$ were calculated via upper dykes and lower gabbros, respectively.

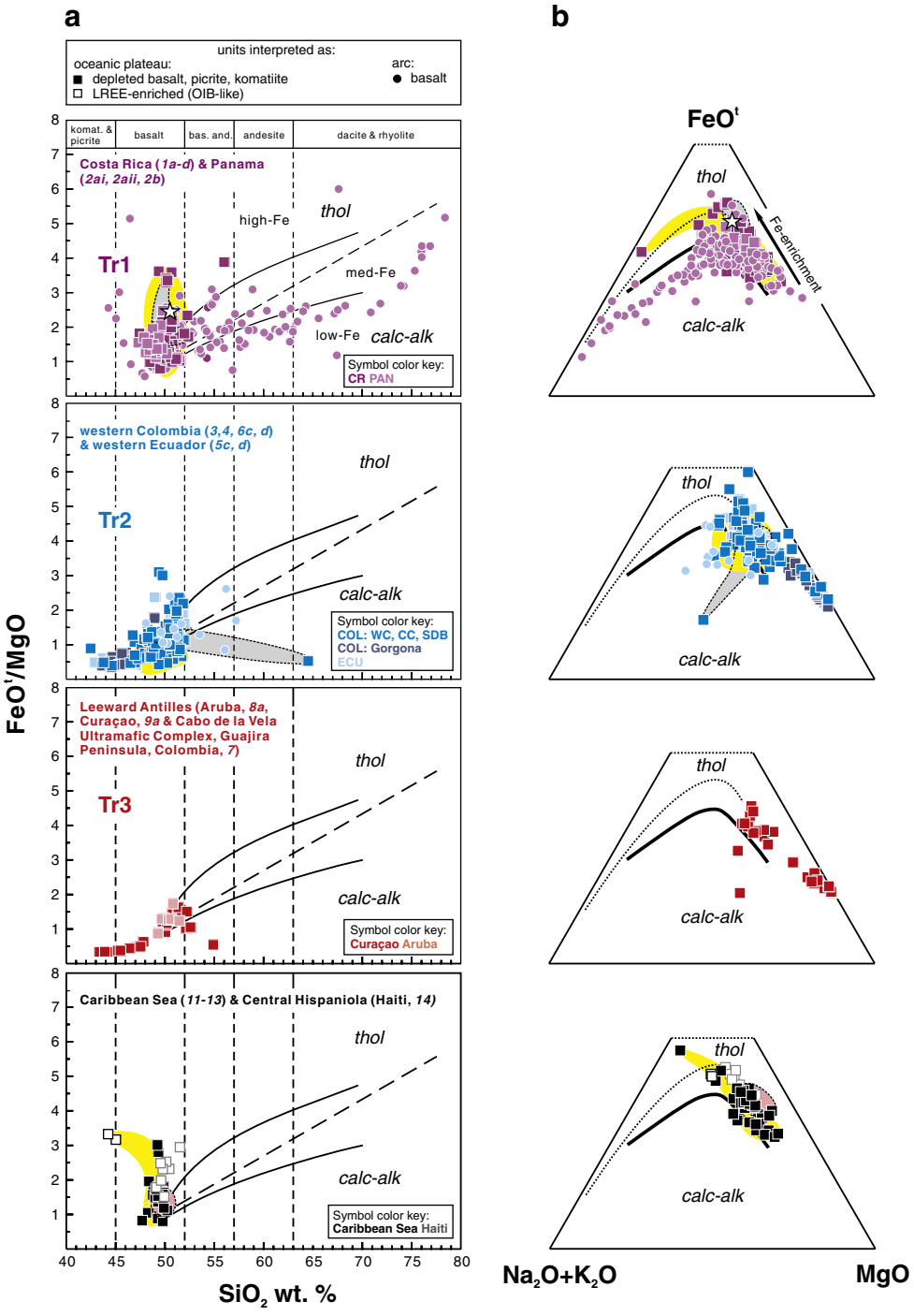

Fig. 4. (a) SiO_2 vs. FeO^t/MgO (Miyashiro, 1974) and (b) AFM (Kuno, 1968; Irvine and Baragar, 1971) relations of lavas and intrusives of PAR units exposed along: Tr1 in Costa Rica and Panama; Tr2 in western Colombia and Ecuador; Tr3 in Aruba and Curacao; and the central and northern segments of the CLIP in the Caribbean Sea and Hispaniola (Haiti, Dominican Republic). Superimposed on (a) are the low-, medium- and high-Fe series of Arculus (2003). In (a) and (b) (top plots) the dashed, gray shaded and yellow regions represent distributions of samples from the 140–110 Ma and 98–82 Ma Nicoya Complex units, respectively; in (a) and (b) (second plots from top), the dashed, gray shaded and yellow regions represent distributions of the 101–98 Ma Volcanic and Amaime formations of the Western Cordillera (Colombia) and the 79–72 Ma Serranía de Baudó Complex, respectively; in (a) and (b) (bottom plots) the dashed, pink shaded and yellow regions represent distributions of 82–80 Ma ODP Leg 165, Site 1001 Caribbean Sea basalts and 82–75 Ma and 56–54 Ma Beata Ridge (central Caribbean Plate) Caribbean Sea lavas and intrusives, respectively. The white stars in (a) and (b) (top plots) represent the only dated sample (AN86, 94.7 ± 0.9 Ma) available from the younger 98–82 Ma Nicoya Complex. In (b) (top plot) one sample from the 98–82 Ma Nicoya Complex and two samples from the 70–39 Ma Chagres–Bayano Arc (Panama) with >70 wt. SiO_2 fall outside of the plot with $FeO^t/MgO > 8$. In (b) (bottom plot) one Duarte Formation intrusive with 54 wt.% SiO2 (described as a diorite) plots outside the plot with $FeO^t/MgO > 8$. See Fig. 11 for SiO_2 vs. FeO^t/MgO relations of circa 95–79 Ma subduction-related, felsic, arc-like intrusives of NW South America and the Greater Antilles. The numbers in italics in brackets beside the region or unit name corresponds to the unit numbers assigned in Fig. 1.

CLIP, respectively. Some post-100 Ma Nicoya lavas and intrusives (yellow shade, Fig. 4a, top plot) also plot along a vertical trend in FeO^t/MgO space alongside 140–110 Ma Nicoya lavas (dashed gray shade, Fig. 4a, top plot); however, we note that only one dated sample (AN86, 94.7 ± 0.9 Ma, white star) from the younger unit has corresponding major and trace element chemistry (one dated circa 88 Ma plagiogranite sample has corresponding chemistry but total oxides <97 wt.% and thus fails our chemical filter, see Section 1 of Supplementary Data). We note

also that the only LREE-enriched lavas or intrusives reflecting lower degree partial melting (e.g., Dumisseau Formation basalts, Loewen et al., 2013) occur in units in the central and northern segments of the Caribbean Plate furthest away from the trench and which received nil subduction additions (see below).

The THI allows iron enrichment or depletion of a given magma series to be quantified (THI > and < 1 are tholeiitic and calc-alkaline respectively). THI is calculated for a magma series and is defined as $Fe_{4.0}/Fe_{8.0}$, where $Fe_{4.0}$ and $Fe_{8.0}$ represent the average FeO^t of magmas with 3–5 and 7–9 wt.% MgO respectively (Zimmer et al., 2010). The applicability of THI is limited by the scarcity of evolved (~4 ± 1 wt.% MgO) PAR igneous rocks; we were only able to reconstruct THI for nine PAR suites. Nonetheless, a plot of THI vs. time (Fig. 5) for units where THI could be calculated demonstrates similarities to trends seen in SiO_2 vs. FeO^t/MgO and AFM space and two important points. First, the oldest post-100 Ma units on the southern side of the Caribbean Plate and NW South America (98–82 Ma components of the Nicoya Complex and the 97–96 Ma Central Cordillera, western Colombia) are clearly tholeiitic, with identical THI of ~1.50. Second, THI decreased with time along the southwestern margin of the CLIP. By 89–85 Ma, THI decreased to <1 as recorded by the Azuero Plateau and to an OPB-like THI of ~1.2 as recorded by the Golfito complex (samples interpreted as plateau by Hauff et al., 2000a,b and as arc by Buchs et al., 2010 represented by a dark purple square and circle respectively, on Fig. 5). The Azuero Plateau records a slightly calc-alkaline THI of 0.97 (Table 3), much lower than average OPB (THI ~ 1.2). Along with other geochemical criteria described below, this feature suggests a hybrid plume-subduction environment of formation, which in the case of the Azuero Plateau, was achieved by 89–85 Ma.

4.2.2. Temporal variations of mantle depletion and degrees of partial melting as recorded by Nb/Yb

Nb is a highly incompatible trace element whereas Yb is a moderately incompatible element and neither is transported by hydrous fluids released from the subducted slab. Consequently, the Nb/Yb ratio decreases as the mantle source region is progressively depleted by melting, so basalts with low Nb/Yb are derived from more depleted mantle than are basalts with higher Nb/Yb (assuming basalts were not generated in equilibrium with garnet). It is not clear from Nb/Yb alone whether source depletion reflects a single event (perhaps at the time that the melt was generated) or the cumulative effects of multiple melting episodes. Fig. 6 shows that OIB and OPB are derived from a mantle source that is less depleted (higher Nb/Yb) than is the source region of MORB (lower Nb/Yb), which is less depleted than the source region of arc basalts like those of the IBMVA (lowest Nb/Yb) (Pearce et al., 2005). Nb/Yb variations with time can thus be used as one perspective on the transition from plume to subduction-modified sources. Thus, we plot Nb/Yb as a proxy of mantle fertility and the relative degree of partial melting vs. time in Fig. 6 to highlight both differences in the degrees of partial melting experienced by pre-vs. post-100 Ma units and to demonstrate that the mantle source was increasingly depleted with time along both the southern and eastern margins of the Caribbean Plate beginning at 100 Ma.

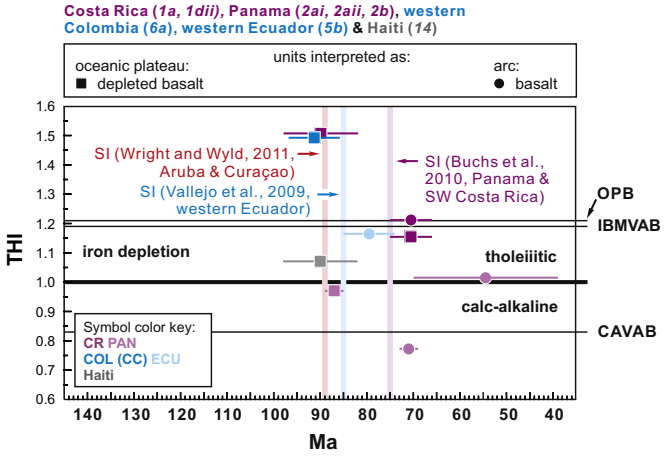

Fig. 5. Tholeiiitic index (THI) (Zimmer et al., 2010) vs. time for post-100 Ma plume- and arc-related units along trace 1 in Costa Rica and Panama and trace 2 in western Ecuador and western Colombia. The faint pink, blue and purple vertical bars demarcate the timing of inferred subduction initiation along: trace 3 in Aruba and Curacao (89 Ma, Wright and Wyld, 2011) on the basis of ages of felsic intrusives of the Aruba Batholith and Curaçao Diorites which intrude the Aruba and Curaçao lava formations (interpreted as CLIP); trace 2 in western Ecuador (85 Ma, Vallejo et al., 2009); and trace 1 in SW Costa Rica and Panama (75 Ma, Buchs et al., 2010), respectively; see text for other details. Note that the Golfito Complex is interpreted as oceanic by Hauff et al. (2000a,b) (purple square) and as arc by Buchs et al. (2010). Unit numbers (in italics in brackets) are as assigned as in Fig. 1.

Overall, Nb/Yb decreases with time from an early plume-like to a later arc-like phase, supporting the idea that the mantle source region was progressively depleted over this tectonomagmatic transition. A similar trend is seen in Nb/Y vs. Zr/Y (see GR Online Supplementary Document and Supplementary Fig. 3). Nb/Yb variations are thus consistent with the PISI model. An important point is that a transition to lower Nb/Yb and hence greater degrees of partial melting is evident by at least 95 Ma (Fig. 6a, b) which suggests that a significant change in the melting regime occurred between 100 and 95 Ma which is at least 6 Ma younger than current interpretations of the transition from plume-to arc (i.e., timing of SI as indicated by faint pink, blue and purple vertical bars in Figs. 5, 6 and subsequent figures). A spatial trend in degrees of partial melting has also been noted by Loewen et al. (2013) who demonstrated a lower degree of partial melting for Dumisseau Formation (Haiti) basalts relative to CLIP lavas further to the south (e.g., those of the Curaçao Lava Formation). As we show below, these trends toward increasing degrees of partial melting with time and according to location (greater degrees of melting in southern and eastern PAR units relative to CLIP in the center and northerly segments of the Caribbean Plate) are mirrored by concomitant trends toward higher subduction contributions with time.

4.2.3. Temporal variations of mantle fugacity as recorded by Ti/V

Ti/V ratios are sensitive to fluctuations in f_{O2} (Shervais, 1982) and the transition from plume to SSZ environment should be reflected in progressively more oxidized mantle. The basis for the Ti/V relation lies in multiple oxidation states of V in magmas (+3, +4, and +5), so V changes from a slightly to a strongly incompatible element as mantle oxygen fugacity increases (Canil, 1997). Ti is +4 and is not redox-sensitive. Low Ti/V (<20) in basalt indicates an oxidized mantle source, as is most commonly associated with SSZ environments, whereas high Ti/V indicates reduced mantle sources akin to those of MORB and OIB (Shervais, 1982). We plot Ti/V versus time for PAR units (Fig. 7) to

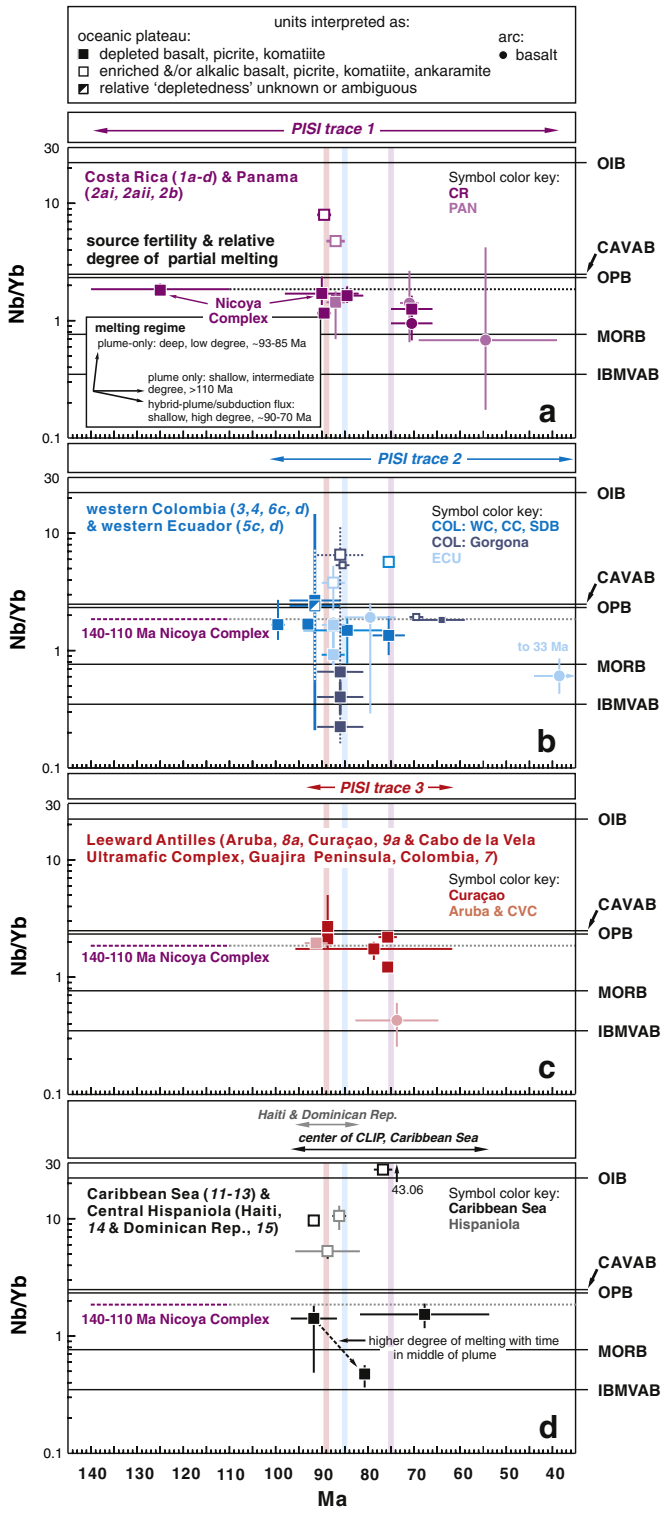

Fig. 6. Mean and range of Nb/Yb vs. time for plume- and arc-related units from this study (squares and circles represent units interpreted as oceanic plateau (OP) and arc, respectively; see top box) from (a) PISI trace 1 in Costa Rica and Panama, (b) PISI trace 2 in western Ecuador and western Colombia, (c) PISI trace 3 in the Leeward Antilles in the Cabo de la Vela Complex, Curaçao and Aruba, and (d) the central and northern segments of the Caribbean Plate in the Caribbean Sea and Central Hispaniola. The small squares in (b) are Gorgona samples of Serrano et al. (2011). References, Nb/Yb ratios and ages for all units in (a)–(d) are provided in Tables 2 and 3 for further correlation. References for the oceanic island basalt (OIB), mid-oceanic ridge basalt (MORB), Central American Volcanic Arc (CAVA) and the Izu Bonin–Marianas Volcanic Arc (IBMVA) are given in Section 3.2. The faint purple, blue and pink vertical bars demarcate the timing of inferred subduction initiation along traces 1, 2 and 3, respectively; see Fig. 5 caption and text for further details. Unit numbers (in italics in brackets) are as assigned as in Fig. 1.

examine if and how the oxygen fugacity in the mantle source changed with time.

Ti/V decreases markedly from OIB (~75) to MORB (~35, Shervais, 1982) and OPB (28, $n = 351$) (Table 3, Fig. 7). Arc basalts typically have Ti/V <20, e.g., the IBM volcanic arc basalts record a mean Ti/V of 16 and range from 8 to 22 ($n = 138$). Quaternary Central American Volcanic arc basalts record a slightly higher mean (21) and a much larger range (10–58) than 'typical' arc basalts, possibly reflecting the inherited plume component in the mantle source of Central American Arc lavas (Gazel et al., 2009, 2011) (Table 3).

Mean Ti/V of most suites along Tr1 (Costa Rica and Panama) is similar to that of the mean Ti/V = 21 of modern Central American Arc basalts (Fig. 7a, Table 3). Although some units exhibit large ranges (e.g., Ti/V ranges from 17 to 39 for depleted basalts of the Azuero Plateau, Table 3), the mean Ti/V generally increases with time until about 70 Ma after which Ti/V drastically falls (Fig. 7a, Table 3). Only the 70–39 Ma Chagres–Bayano Arc of Panama shows a significantly lower Ti/V of 15, similar to that of IBMVA basalts (elevated Ti/V of 60 and 40 are for a single Tortugal basalt of unknown 'depletedness' and for the enriched Azuero Plateau basalt suite, $n = 2$, Table 3). Tr2 Ti/V increases with time in a similar manner to Tr1 if one considers only the mean Ti/V of Colombian units but the scatter in Ti/V of 90–80 Ma Colombia lavas complicates the evolution in general (Fig. 7b). Variability here is again dominated by large ranges of Ti/V in Gorgona lavas. For example, depleted Gorgona basalts and komatiites display similar means of Ti/V = 16, identical to IBMVA basalts and Gorgona picrites exhibit the lowest mean Ti/V of all units (12) (Table 3) similar to Ti/V of boninites. Ecuador PAR sequences evolve to low, arc-like Ti/V by ~80 Ma, when the Rio Cala arc formed (Fig. 7b). Ti/V for Tr3 PAR sequences shows little change, ranging only from ~18–20 for all 5 sequences examined (Fig. 7c). CLIP sequences away from the three PISI traces appear to decrease with time but never reach arc-like values <20 (Fig. 7d).

Unfortunately, there are no V analyses available for the 140–110 Ma Nicoya OPB but it is important to note that Ti/V is much higher than typical arc basalts (<20) and quite variable away from the three traces (Fig. 7d). For example, mean values range from ~70 for enriched basalts to ~25 for depleted dolerites from the Beata Ridge in the center of the Caribbean Plate (Table 3). Similarly, lavas of the Dumisseau Formation, Haiti record Ti/V that range from 33 to 63 (Table 3). As these values are much higher than those of typical arc basalts this indicates derivation from a mantle source that was more reduced than that supplying arc magmas.

That Ti/V remained relatively high along Tr1 and Tr2 (generally higher than 20) but decreased erratically to lower, arc-like values <20 especially after 75 Ma may indicate that the plume mantle source was not strongly oxidized by subduction until ~20 Ma after the main plume phase. The PISI model does not readily explain why oxidation took so long but is possibly the result of extended plume contributions until ~75 Ma, after which plume contributions appear to rapidly decrease (e.g., Fig. 3). We note that even modern Central American Arc lavas have slightly higher Ti/V than expected for arcs. Perhaps the plume continued to supply reduced mantle which buffered the oxygen fugacity of the evolving mantle source.

4.2.4. Temporal variations of subduction additions: Ba/Th, Ba/Nb, and Th/Nb

Hydrous fluids released from the subducted slab carry fluid-mobile elements (such as Rb, Ba, Sr, and Pb) up and into the overlying mantle. Because the upper surface of the slab is progressively heated as it sinks to greater depth, subducted sediments carried to depths of 100 km or more can melt, transporting other incompatible trace elements such as Th into the overlying mantle (Elliott et al., 1997). Fluid and melt are sometimes referred to as "shallow" and "deep" subduction components, respectively, and together comprise the total subduction component that is released from the subducting plate. Fluids and melts released

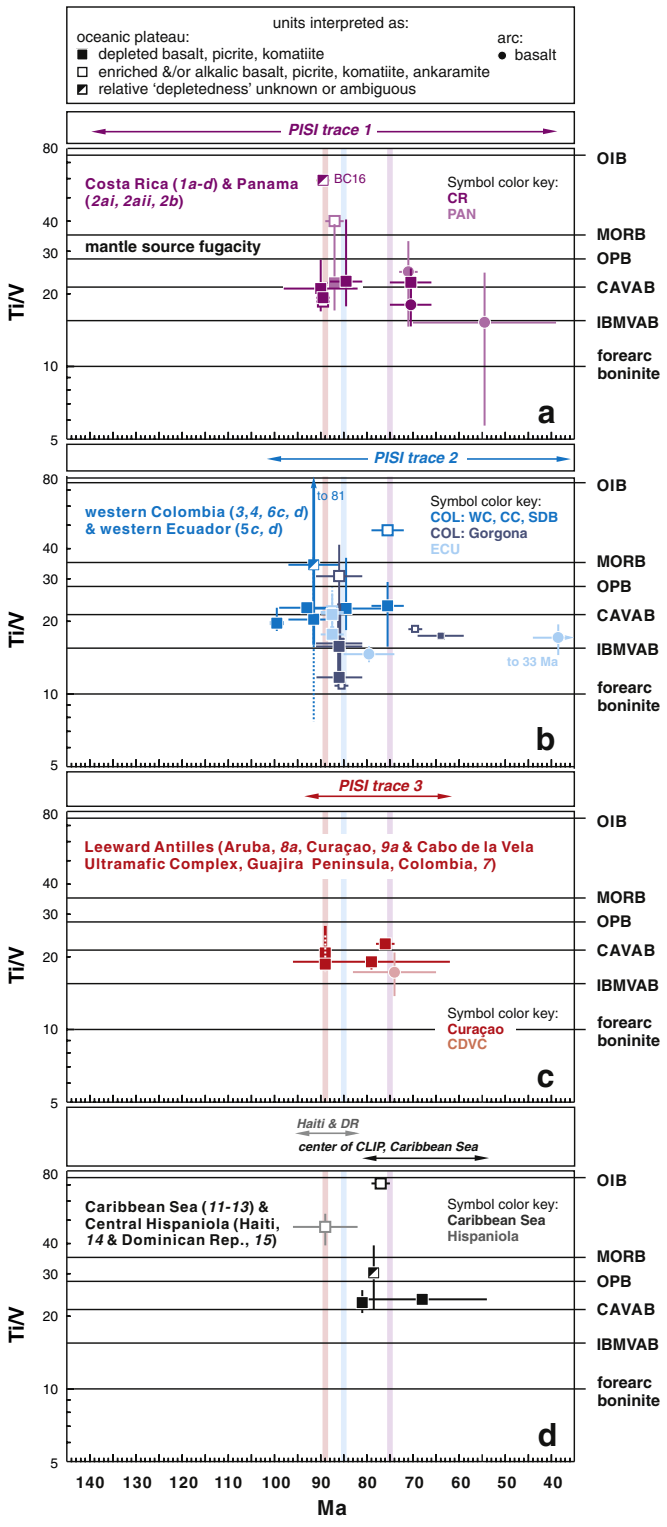

Fig. 7. Mean and range of Ti/V vs. time for plume- and arc-related units from this study (squares and circles represent units interpreted as oceanic plateau (OP) and arc, respectively; see top box) from (a) PISI trace 1 in Costa Rica and Panama, (b) PISI trace 2 in western Ecuador and western Colombia, (c) PISI trace 3 in the Leeward Antilles in the Cabo de la Vela Complex, Curaçao and Aruba, and (d) the central and northern segments of the Caribbean Plate in the Caribbean Sea and Central Hispaniola. The small squares in (b) are Gorgona samples of Serrano et al. (2011). References, Ti/V and ages for all units in (a)–(d) are provided in Tables 2 and 3 for further correlation. References for the oceanic island basalt (OIB), mid-oceanic ridge basalt (MORB), Central American Volcanic Arc (CAVA) and the Izu Bonin–Marianas Volcanic Arc (IBMVA) are given in Section 3.2. The faint purple, blue and pink vertical bars demarcate the timing of inferred subduction initiation along traces 1, 2 and 3, respectively; see Fig. 5 caption and text for further details. Unit numbers (in italics in brackets) are as assigned as in Fig. 1.

from the sinking slab ascend into the overlying mantle, metasomatizing it and causing it to melt. Ratios of fluid- and melt-mobile Ba and melt (only)-mobile Th with trace elements sensitive to mantle composition such as Nb or Yb determined in basalts can be used to monitor this addition (Pearce et al., 2005). To better illustrate trends in subduction additions of post-100 Ma units described above, we plot Ba/Th (shallow subduction additions), Th/Nb (deep subduction additions) and Ba/Nb (total subduction additions) (Elliott et al., 1997; Pearce et al., 2005) vs. time in Figs. 8–10. As some studies suggest that Ba is an unreliable petrogenetic indicator due to its potential mobility during hydrothermal alteration, we discuss why this appears not to be the case in Supplementary Section 1 of the GR Online Supplementary Document.

The variation of these 'subduction-sensitive' trace element ratios in post-100 Ma PAR units can be compared spatially and temporally to those in the center and northern segments of the Caribbean Plate and with the 140–110 Ma Nicoya Complex, the latter two of which received no discernible subduction inputs apart perhaps from the 82–80 Ma Caribbean Sea basalts. For example, the ODP Leg 165 basalts are somewhat anomalous recording a mean Ba/Th similar to IBM volcanic arc basalts and which range to values higher than mean Central American Arc lavas (Fig. 8d). Apart from these Leg 165 basalts, the shallow subduction component in central and northern Caribbean Plate igneous rocks is limited, with mean Ba/Th ~25–115, about the range expected for global MORB, OPB, and OIB (Fig. 8d). Apart from the Leg 165 basalts and post-80 Ma Beata Ridge dolerites which show Ba/Nb that ranges to values intermediate to that of OIB and arc basalts (Fig. 9d) the total subduction component of Caribbean Sea and Hispaniola basalts is similarly modest, with Ba/Nb ~2–28, again mostly similar to what is expected for global MORB, OPB, and OIB (Fig. 9d). Little evidence of a deep subduction component is observed, with Th/Nb <0.1, again mostly similar to what is expected for global MORB, OPB, and OIB (Fig. 10d). Similarly, the Ba/Th, Ba/Nb and Th/Nb of 140–110 Ma Nicoya Complex basalts are very similar to OPB and OIB (Figs. 8a, 9a, 10a) and record no evidence of subduction modification. The similarity in the older Nicoya Complex basalts with OPB is also apparent in N-MORB normalized plots (Supplementary Fig. 4). The aforementioned ranges provide a useful baseline for comparison with PAR sequences along Tr1, Tr2, and Tr3.

In general, most volcanic rocks of post-100 Ma PAR units in Tr1 and Tr2 display evidence of shallow and total subduction additions as gauged by elevated Ba/Th and Ba/Nb (Figs. 8, 9); conversely, post-100 Ma units in Tr3 in the Leeward Antilles and the northern and central segments of the Caribbean Plate generally do not. Exceptions include the Aruba Lava Formation basalts which have mean Ba/Th ~156 and Ba/Nb ~11 (Table 3) similar to similarly-aged units along Tr1 and Tr2 and the (probably ~70 Ma) Cabo de la Vela 'latest stage' dykes which have Ba/Th and Ba/Nb higher than Central American Arc basalts (Figs. 8d, 9d). Tr1 PAR units have Ba/Th (~100–200) intermediate to OIB and IBM volcanic arc basalts until ~70 Ma when Ba/Th rose to modern day Central American Arc values of 200–600; Ba/Th reached 600–800 by the end of the Cretaceous in the Chagres–Bayano arc and remains high in the modern Central American Arc (Fig. 8a, Table 3). The total subduction component (Ba/Nb) began to increase above values expected for OIB–OPB (~8) by 85 Ma (Ba/Nb of ~10–20) and rose to ~20–60 by ~70 Ma (Fig. 9a, Table 3). Ba/Nb for Chagres–Bayano arc lavas is indistinguishable from that for modern arc lavas from Central America or IBM arc basalts (Fig. 9a). Evidence of the deep subduction component (Th/Nb) rose more slowly, exceeding baseline values for MORB, OIB, and OPB by ~70 Ma (Fig. 10a).

The record of subduction inputs preserved in Tr2 PAR sequences suggests that this mantle source was modified earlier by subduction inputs and at a faster rate than was the Tr1 source (e.g., compare Figs. 8a and 9a with 8b and 9b). Although Colombia PAR sequences scatter widely, the oldest, circa 100 Ma western Colombia PAR sequence (western Cordillera) has mean Ba/Th (shallow subduction inputs) much higher (~650) than plume mantle (OIB and OPB, ~70–90 and 140–110 Ma Nicoya Complex, ~100) and even higher than Central

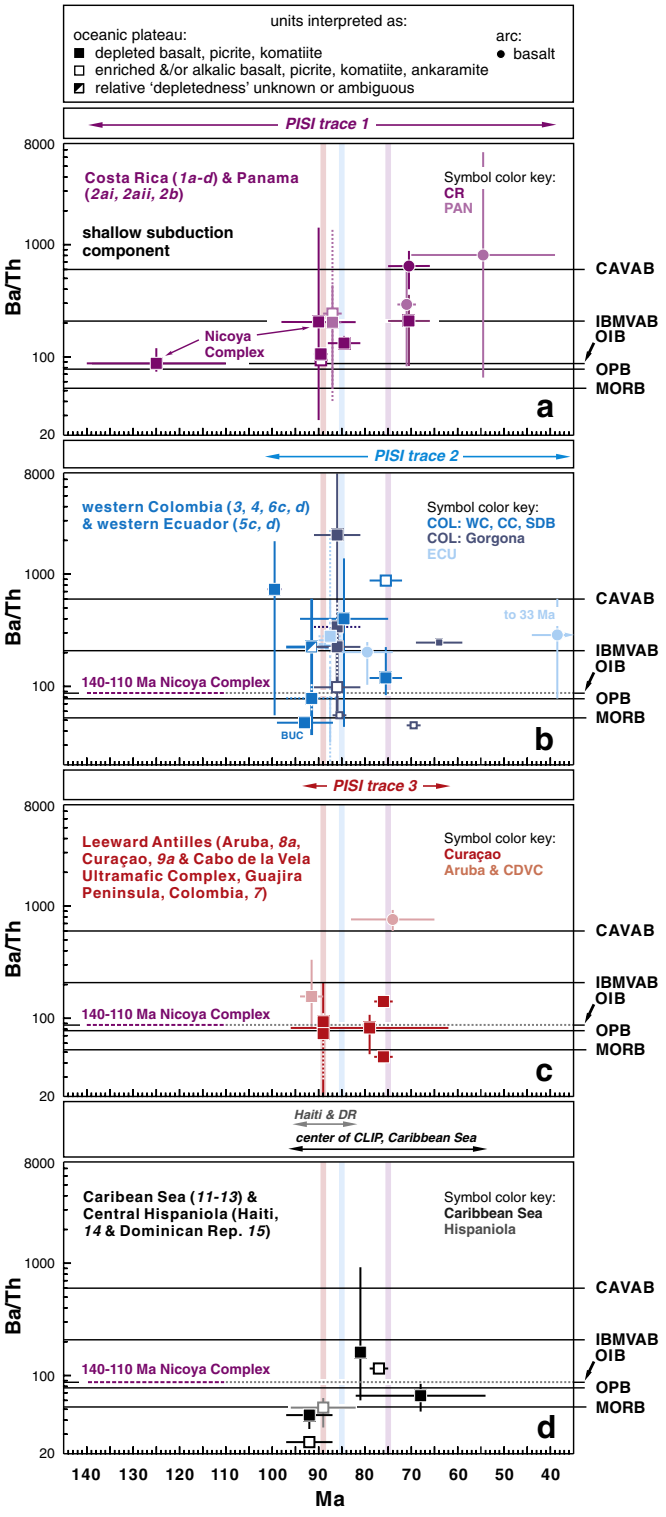

Fig. 8. Mean and range of Ba/Th vs. time for plume- and arc-related units from this study (squares and circles represent units interpreted as oceanic plateau (OP) and arc, respectively; see top box) from (a) PISI trace 1 in Costa Rica and Panama, (b) PISI trace 2 in western Ecuador and western Colombia, (c) PISI trace 3 in the Leeward Antilles in the Cabo de la Vela Complex, Curaçao and Aruba, and (d) the central and northern segments of the Caribbean Plate in the Caribbean Sea and Central Hispaniola. The small squares in (b) are Gorgona samples of Serrano et al. (2011). References, Ba/Th and ages for all units in (a)–(d) are provided in Tables 2 and 3 for further correlation. References for the oceanic island basalt (OIB), mid-oceanic ridge basalt (MORB), Central American Volcanic Arc (CAVA) and the Izu Bonin–Marianas Volcanic Arc (IBMVA) are given in Section 3.2. The faint purple, blue and pink vertical bars demarcate the timing of inferred subduction initiation along traces 1, 2 and 3, respectively; see Fig. 5 caption and text for further details. Unit numbers (in italics in brackets) are as assigned as in Fig. 1.

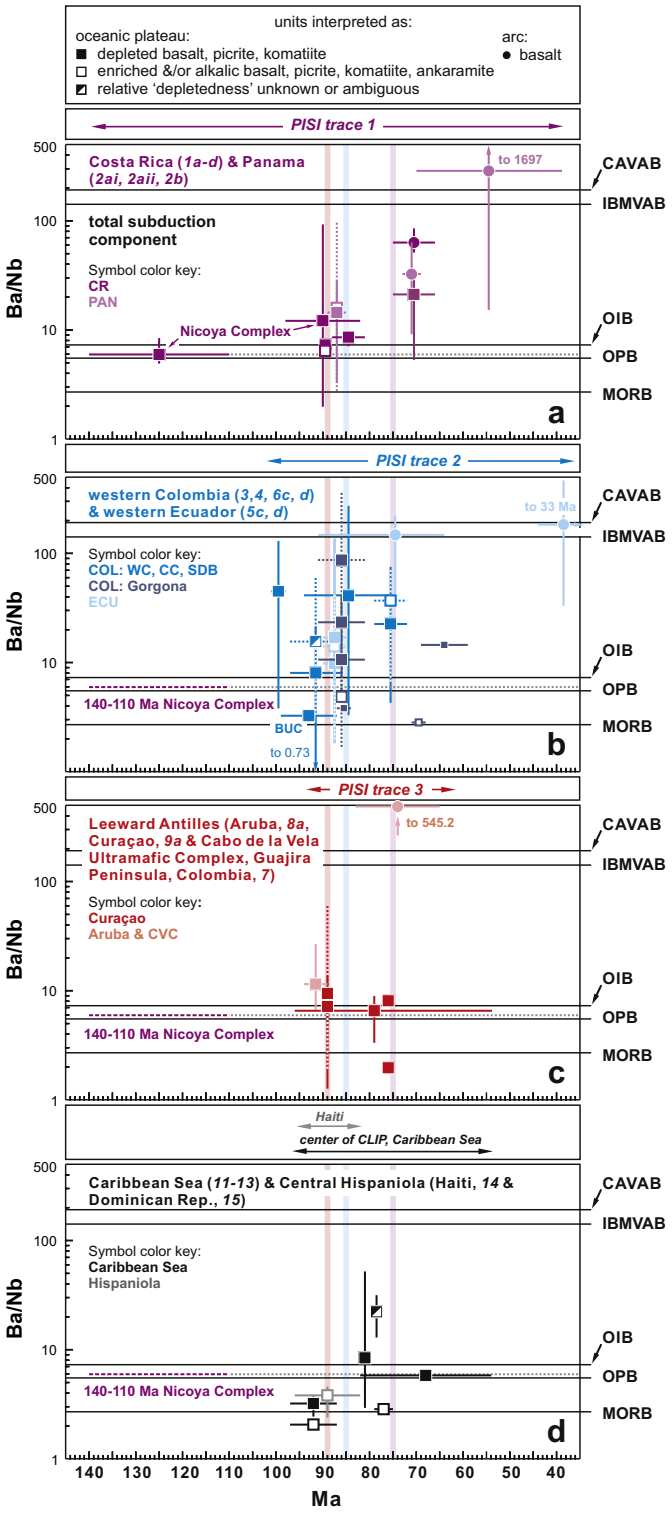

Fig. 9. Mean and range of Ba/Nb vs. time for plume- and arc-related units from this study (squares and circles represent units interpreted as oceanic plateau (OP) and arc, respectively; see top box) from (a) PISI trace 1 in Costa Rica and Panama, (b) PISI trace 2 in western Ecuador and western Colombia, (c) PISI trace 3 in the Leeward Antilles in the Cabo de la Vela Complex, Curaçao and Aruba, and (d) the central and northern segments of the Caribbean Plate in the Caribbean Sea and Central Hispaniola. The small squares in (b) are Gorgona samples of Serrano et al. (2011). References, Ba/Nb and ages for all units in (a)–(d) are provided in Tables 2 and 3 for further correlation. References for the oceanic island basalt (OIB), mid-oceanic ridge basalt (MORB), Central American Volcanic Arc (CAVA) and the Izu Bonin–Marianas Volcanic Arc (IBMVA) are given in Section 3.2. The faint purple, blue and pink vertical bars demarcate the timing of inferred subduction initiation along traces 1, 2 and 3, respectively; see Fig. 5 caption and text for further details. Unit numbers (in italics in brackets) are as assigned as in Fig. 1.

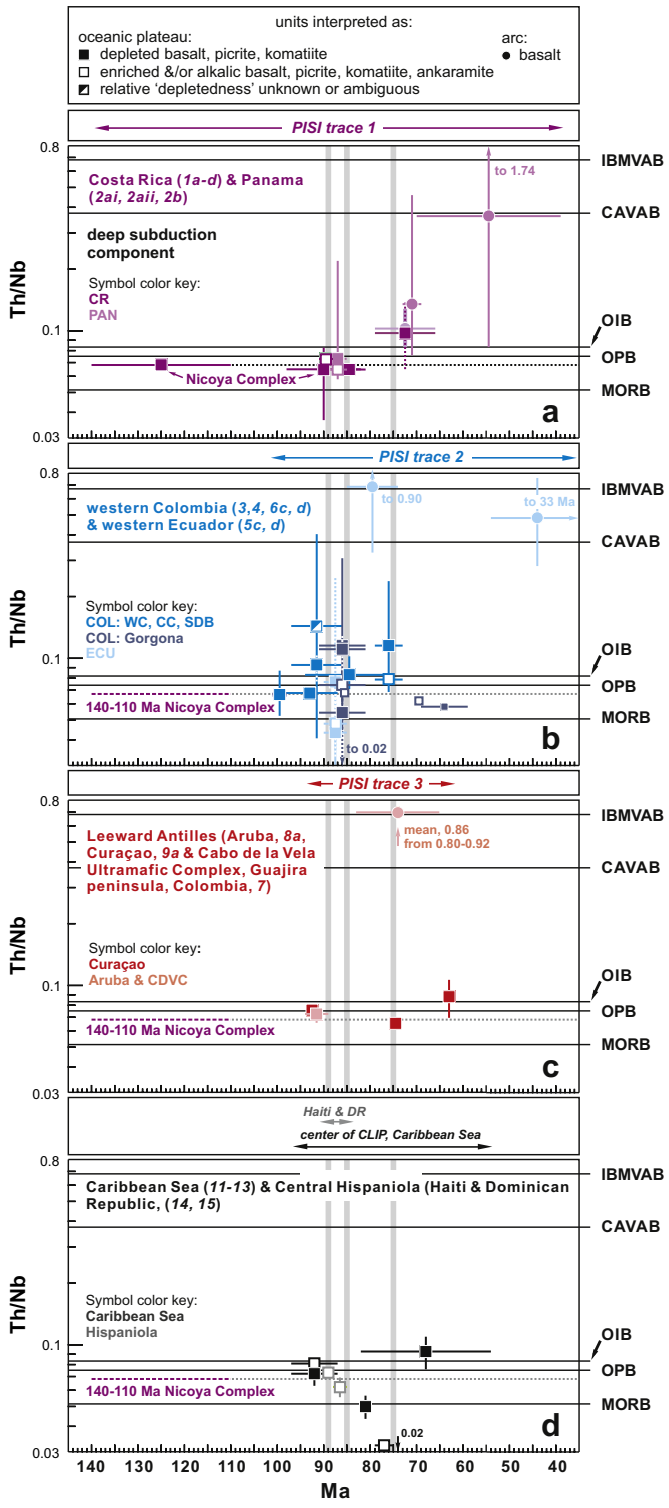

Fig. 10. Mean and range of Th/Nb vs. time for plume- and arc-related units from this study (squares and circles represent units interpreted as oceanic plateau (OP) and arc, respectively; see top box) from (a) PISI trace 1 in Costa Rica and Panama, (b) PISI trace 2 in western Ecuador and western Colombia, (c) PISI trace 3 in the Leeward Antilles in the Cabo de la Vela Complex, Curaçao and Aruba, and (d) the central and northern segments of the Caribbean Plate in the Caribbean Sea and Central Hispaniola. The small squares in (b) are Gorgona samples of Serrano et al. (2011). References, Th/Nb and ages for all units in (a)–(d) are provided in Tables 2 and 3 for further correlation. References for the oceanic island basalt (OIB), mid-oceanic ridge basalt (MORB), Central American Volcanic Arc (CAVA) and the Izu Bonin–Marianas Volcanic Arc (IBMVA) are given in Section 3.2. The faint purple, blue and pink vertical bars demarcate the timing of inferred subduction initiation along traces 1, 2 and 3, respectively; see Fig. 5 caption and text for further details. Unit numbers (in italics in brackets) are as assigned as in Fig. 1.

American Arc lavas (Fig. 8b, Table 3). 90 Ma Colombian units have Ba/Th that are mostly higher than OIB and OPB and Ecuador units have Ba/Th (~200) twice that of background OIB–OPB–MORB (<100) (Fig. 8b, Table 3). Total subduction inputs monitored by Ba/Nb are also mostly much higher for Tr2 PAR sequences (10–200) than plume mantle (<8; Fig. 9b).

Tr3 PAR sequences generally have mean Ba/Th, Ba/Nb and Th/Nb that scatter around baseline values for plume mantle (OIB, OPB, 140–110 Ma Nicoya Complex), although Aruba Lava Formation basalts exhibit Ba/Th and Ba/Nb higher than plume and similar to post-100 Ma Tr1 and Tr2 units (Figs. 8–10).

In the GR Online Supplementary Document we also provide N-MORB- and primitive mantle-normalized plots (Supplementary Figs. 4, 5) to demonstrate that many lavas of units interpreted as plateau exhibit high, arc-like LILE/HFSE ratios consistent with a SSZ formation. Additionally as discussed in Section 5, circa 100–80 Ma felsic intrusives that cut slightly older units interpreted as plateau exhibit unequivocal subduction additions and HFSE depletions indicative of a supra-subduction zone (SSZ) environment.

4.3. Isotopic constraints

We use isotopic data to evaluate whether or not the mantle source for PAR sequences can be linked to the mantle plume responsible for CLIP formation, which is widely accepted to be the Galapagos Plume (Duncan and Hargraves, 1984; Hauff et al., 1997). Sr isotopic compositions are easily affected by seafloor weathering and low grades of metamorphism, so we neglect this to focus on alteration-resistant Nd and Pb systems. Hf isotopic data for PAR sequences would also be useful but there is little of this available yet. For these reasons, we focus on $^{143}Nd/^{144}Nd$ and $^{206}Pb/^{204}Pb$ that has been corrected for radiogenic growth after eruption. Plots of initial, age-corrected $^{206}Pb/^{204}Pb$ versus $^{143}Nd/^{144}Nd$ for the Caribbean igneous rocks of interest are shown on Fig. 11, along with fields defined by Quaternary lavas from the Galapagos plume (GP in Fig. 11a) and Central American (volcanic) arc (CAVA in Fig. 11a). Modern plume and arc lavas occupy similar fields, suggesting a similar mantle source today. The modern Galapagos field is corrected for 90 Ma of radiogenic growth (dashed fields in Fig. 11) for comparison with ~90 Ma CLIP and PAR sequences. Isotopic data for lavas from the central Caribbean, away from subduction influences, show similar compositions, although ODP Site 1001 lavas come from a more depleted source (Fig. 11g). Igneous rocks from Tr1, Tr2, and Tr3 mostly fall within the age-corrected field for Galapagos plume lavas, which is consistent with the interpretation that these melts were derived from a broadly similar mantle source.

5. Discussion

Below we explore the implications of our compiled data for Late Cretaceous magmatic evolution in the SW Caribbean for testing the PISI model. First we summarize the tectonic significance of the geochemical and isotopic insights presented in Section 4 as well as the significance of felsic, subduction-related intrusions in the Leeward Antilles and NW South America. We then compare the Caribbean PISI sequences with other SI examples. Because the PISI model predicts a continuous evolution from plume- to arc-igneous sequences, we discuss the key question of whether or not there is a hiatus between Late Cretaceous plume and arc igneous activity. We then discuss the advantages of the PISI model for understanding the Late Cretaceous tectonic evolution of this region and outline a critical test of competing models for the tectonic evolution of this region: the presence or absence of a hiatus between early plume and late arc magmatic successions. Finally, we briefly consider how documenting the Caribbean PISI model advances our understanding of how, if not when, plate tectonics began on Earth.

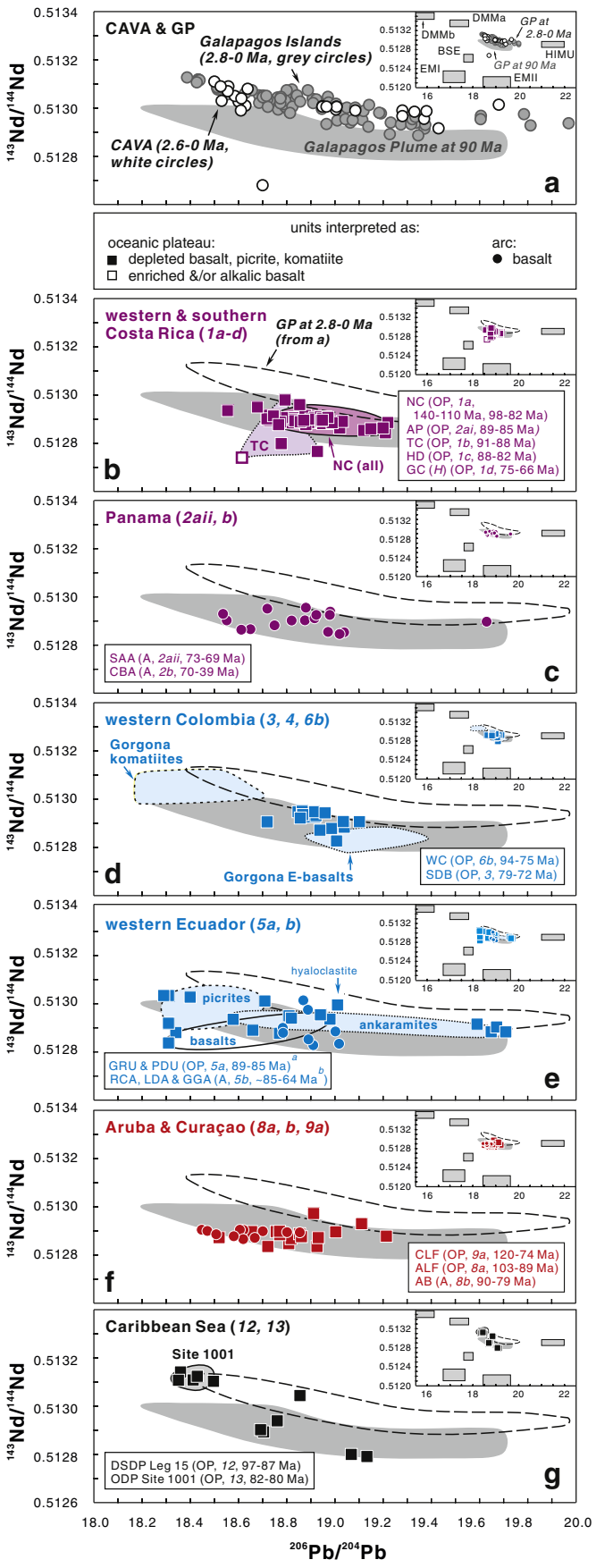

5.1. Synopsis of geochemical and isotopic constraints

We recognize three coterminous PISI traces, each ~1000 km long, along the southern margins of the Caribbean Plate and NW South America where ~100–90 Ma plume-dominated tectonic environments evolved into convergent margins during Late Cretaceous time. The isotopic data indicate that Caribbean igneous rocks were derived from a mantle source similar to that of the modern Galapagos plume, and the combined geochemical and geochronological data provide insights about when during the Late Cretaceous this mantle source began to be modified by subducted inputs. We know that a subduction zone existed as early as 89 Ma along Tr3 because calc-alkaline plutonic rocks of this age are known from Aruba and Curaçao (e.g., Wright and Wyld, 2011). PAR sequences changed throughout Late Cretaceous time from strongly tholeiitic suites expected for OPB toward increasingly calc-alkaline, arc-like compositions (Figs. 4, 5). Nb/Yb ratios show that mantle sources became increasingly depleted and arc-like with time for Tr1; Tr2 Nb/Yb variations with time are complex (Fig. 6). Mantle oxidation state as monitored by Ti/V decreases to lower, arc-like values but only after 80–70 Ma, indicating that the plume mantle source was not strongly oxidized by subduction until ~20 Ma after the main plume phase (Fig. 7). Tr1 and Tr2 igneous rocks show increasing contributions of shallow and total subduction components as gauged by elevated Ba/Th and Ba/Nb, respectively (Figs. 8, 9). Tr1 PAR units have initial (~95 Ma) mean Ba/Th of ~100–200, intermediate to that of OIB/OPB and IBMVA basalts or similar to IBMVA basalts and by ~70 Ma, Ba/Th had risen to 200–600, transitional to IBMVA and Central American Arc basalts; Ba/Th reached 600–800 by the end of the Cretaceous in the Chagres–Bayano Arc and remains high in the modern Central American Arc. The total subduction component (Ba/Nb) began to increase above values expected for OIB–OPB earlier, rising to ~10–20 by 85 Ma and 20–60 by ~70 Ma. Evidence of the deep subduction component (Th/Nb) in Tr1 lavas rises exceeds baseline values for MORB, OIB, and OPB by ~70 Ma (Fig. 10). The record of subduction inputs in Tr2 PAR sequences shows that this mantle source was modified earlier by subduction inputs than was the Tr1 source. Colombia PAR sequences scatter widely but have Ba/Th (shallow subduction inputs) that are mostly and sometimes much higher than plume mantle (OIB, OPB and 140–110 Ma Nicoya Complex) by 90 Ma. Ecuador sequences also have high Ba/Th (~200), about double that of background OIB–OPB–MORB values (<100) and higher than IBMVA basalts. Total subduction inputs monitored by Ba/Nb are also mostly much higher for Tr2 PAR sequences (10–200) than plume mantle (<8). The geochemical data show that early plume-related OPB igneous activity in the SW Caribbean Plate evolved rapidly into arc igneous activity before the end Cretaceous consistent with a general PISI model.

Fig. 11. Initial, age-corrected $^{206}Pb/^{204}Pb$ vs. $^{143}Nd/^{144}Nd$ of (a) lavas of the 2.8–0 Ma Galapagos Islands (White et al., 1993) (or Galapagos Plume, GP) and basalts of the Quaternary Central American Volcanic A (CAVA) (as compiled by Jordan et al., 2012) versus (c–g) Late Cretaceous to Eocene southern Caribbean plume- and arc-related (PAR) units. Mantle domains in the inset (BSE, DMMa, DMMb, EMI, EMII, HIMU) are from Zindler and Hart (1986) and the field for the GP at 90 Ma is from Hauff et al. (2000b). Abbreviations and references for the Caribbean PAR units: (b), NC, Nicoya Complex (140–110 Ma, Hoernle et al., 2004; 98–82 Ma, Sinton et al., 1997; Hauff et al., 2000a,b); (c) DSDP Leg 15 (Hauff et al., 2000b; ODP Site 1001, Kerr et al., 2009); (c) CBA, Chagres–Bayano Arc (Wegner et al., 2011); SAA, Sona–Azuero Arc (Lissinna, 2005; Wegner et al., 2011); (d) the fields for Gorgona komatiites and enriched- (E-) basalts are from Hauff et al. (2000b) based on references therein; SDB, Serranía de Baudó and WC, Western Cordillera (Hauff et al., 2000b); (e) GRU, Guaranda Unit, PDU, Pedernales Unit (Mamberti et al., 2003); RCA, Rio Cala Arc, LDA, La Derecha Arc, GGA, Guaragua Arc (Allibon et al., 2008); (f) AB, Aruba Batholith and ALF, Aruba Lava Formation (White et al., 1999); CLF, Curaçao Lava Formation (Hauff et al., 2000b). DSDP Leg 15 (Hauff et al., 2000b); ODP Site 1001 (Kerr et al., 2009). Superscripts: a, the GRU and PDU are considered as circa 90–85 Ma correlatives of the Pallatanga Unit and the Piñon Formation and other similarly aged western Ecuador oceanic plateau units (see Mamberti et al., 2003); b, whereby the RCA represents arc constructed upon the Pallatanga Unit (interpreted as CLIP, see Figs. 1 and 2 and Mamberti et al., 2003; Vallejo et al., 2009) the LDA and GGA are interpreted as arc materials constructed upon the Piñon Formation which is considered to represent 90–85 Ma oceanic plateau analogous to the Pallatanga Unit and other similar units in western Ecuador (see Mamberti et al., 2003 and Allibon et al., 2008). Units numbered as in Fig. 1.

5.2. Significance of 99–79 Ma arc-related, felsic granitoid suites: Implications for the timing of subduction initiation

While absent from Tr1, 99–79 Ma arc-related, felsic 'granitoid' units intrude ~100–80 Ma oceanic plateau basement in Tr2 (western Ecuador, western Colombia) and Tr3 (Aruba and Curaçao) (Fig. 1 and listed with ages in Table 2; see also the GR Online Supplementary Document). In Aruba and Curaçao, CLIP sequences are intruded by 90–79 Ma and 87–85 Ma felsic, arc-related plutonic rocks, respectively (White et al., 1999; van der Lelij et al., 2010; Wright and Wyld, 2011; Aruba Batholith, Curaçao Diorites, Table 2). In western Colombia, the 95–86 Ma Antioquia and the 93–89 Ma Buga batholiths intrude ~100–80 Ma oceanic plateau basement in the Central and Western Cordilleras, respectively (Villagómez et al., 2011). Further north, in the Western Cordillera of Colombia, ~91 Ma pegmatites of the Bólivar Ultramafic Complex (BUC) (Kerr et al., 2004; Villagómez et al., 2011) intrude basement interpreted as CLIP. Although the BUC is also interpreted as plateau (Kerr et al., 2004), the chemical composition of BUC andesites is similar to contemporaneous felsic intrusives elsewhere in western Colombia and in Ecuador, Aruba and Curaçao (see below). In western Ecuador the 87–81 Ma arc-related Pujilí Granite is entrained in a tectonized zone of the 90–85 Ma Pallatanga Unit interpreted as CLIP (Vallejo et al., 2006, 2009).

Some workers consider these plutonic rocks as tonalite–trondhjemite–granodiorite-like or adakitic units (e.g., Wright and Wyld, 2011), reflecting the consensus that these are subduction-related. These plutonic felsic rocks show calc-alkaline affinities (Fig. 12a, b), and are most reasonably interpreted as juvenile arc granitoids (Fig. 12c). An arc origin is further supported by marked HFSE-depletions (Supp. Fig. 6) but the only felsic unit that exhibits a convincing origin from a garnet-bearing protolith is the youngest 87–81 Ma Pujilí Granite (western Ecuador) with chondritic HREE and Y concentrations (Supplementary Fig. 6c, d). Furthermore, all of the aforementioned felsic suites fall within the range of REE patterns for 73–69 Ma Sona–Azuero Arc (Panama) granites (Supplementary Fig. 6i); show similar N-MORB patterns as the younger Panamanian granites (Supplementary. Fig. 6b–j); and are identical to younger 75–39 Ma granites of the Panamanian segment of the early Central American Volcanic arc system in Y vs. Nb space, including Bólivar Ultramafic Complex felsic pegmatites and felsite dykes (Fig. 12b). Chondrite-normalized REE plots and N-MORB normalized incompatible element patterns of Bólivar Ultramafic Complex basalts, pegmatites and felsite dykes are provided in Supplementary Fig. 7.

As some of the felsic arc units pre-date the lower range of the associated plateau unit, this demonstrates that these are not always intrusive but rather co-magmatic (e.g., as in Curaçao, see Table 2). An unambiguous arc origin is supported by the marked HFSE-depletions and LILE enrichments and as these felsic suites usually only slightly post-date the CLIP basement they cut, these felsic plutons provide evidence that SI quickly followed plume emplacement, consistent with PISI.

5.3. Comparison of Caribbean PISI sequences and other SI examples

The Caribbean PISI example shares significant similarities with other examples of subduction initiation, but association with a plume makes it unique. One important similarity is that the oldest units of both Caribbean PISI and IBM SI sequences show no subduction input; arc-like affinities appear only after a few million years (Ishizuka et al., 2011). The MORB-like affinities of lower basaltic units of many Tethyan-type ophiolites and Izu-Bonin forearc sequences are compositionally distinct from overlying arc-like units and this dichotomy has led some workers to infer two tectonic environments: first at a mid-ocean ridge and second at a volcanic arc (see Whattam and Stern, 2011 and references therein). For example, IBM forearc basalts (Reagan et al., 2010) comprising the inner slope of the Izu-Bonin trench were originally interpreted as trapped, older Philippine Sea MOR crust (DeBari et al., 1999). A similar scenario has been posited for SW Pacific ophiolites but with the lower MORB-like sequences representing trapped backarc basin crust (see Whattam, 2009). Explanations for the Late Cretaceous evolution of the Central American Arc are similar,

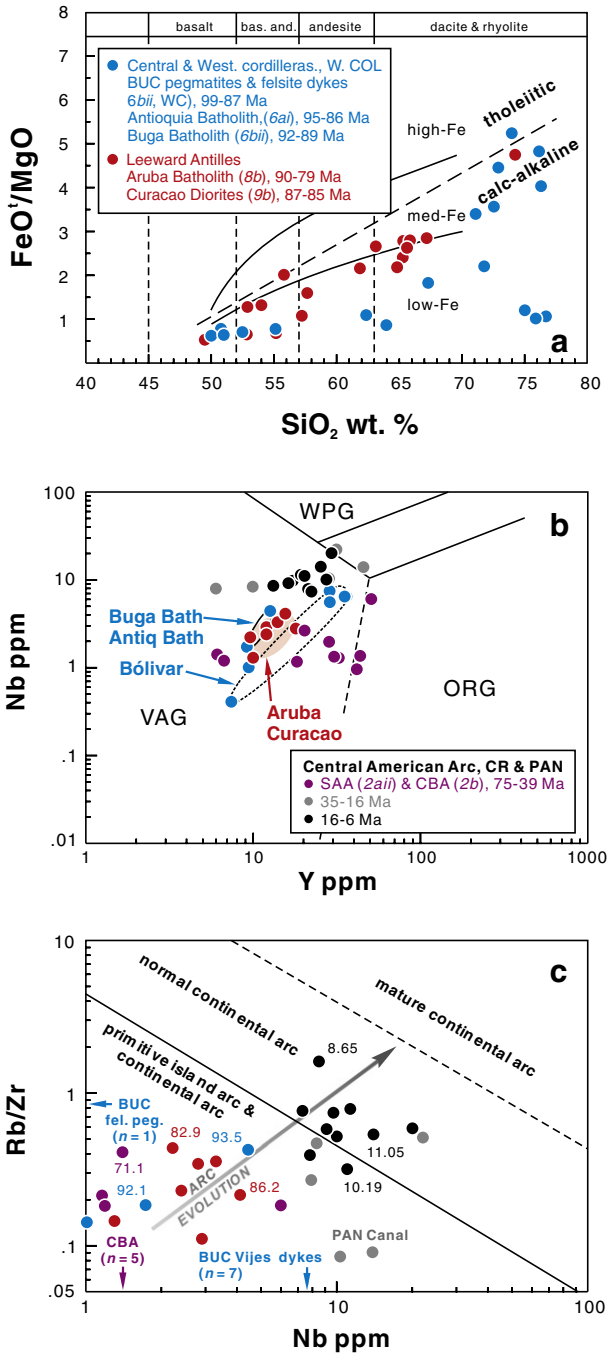

Fig. 12. (a) SiO_2 vs. FeO^t/MgO, (b) Y vs. Nb (a) and (c) Nb vs. Rb/Zr plots of circa 95–79 Ma subduction-related, felsic, arc-like intrusives of NW South America and the Greater Antilles, 99–87 Ma Bólivar Ultramafic Complex (BUC), Western Cordillera, western Colombia and younger 75–6 Ma granitoids of the Central American Volcanic Arc in Costa Rica (CR) and Panama (PAN). The subalkaline discrimination plot in (a) is from Miyashiro (1974) and the subfields of high-, medium- and low-Fe are from Arculus (2003). Plots and fields in (b) and (c) are from Pearce et al. (1984) and Brown et al. (1984), respectively. All data in (b) are of samples with 65–75 wt.% SiO_2 apart from two BUC Vijes dykes with 76 wt.% SiO_2. References for all 35–16 Ma Costa Rican and Panamanian granitoids are from Kessler et al. (1977), Drummond et al. (1995 and references listed therein), Wörner et al. (2009) and Wegner et al. (2011). References for the 95–79 Ma felsic plutonic units are listed in Table 2. Other abbreviations in (b): CBA, Chagres–Bayano Arc (Panama), CR, Costa Rica, PAN, Panama, ORG, ocean ridge granite, SAA, Sona–Azuero Arc (Panama) VAG, volcanic arc granite, WPG, within-plate granite. Numbers beside symbols in (c) represent ages in Ma. Units numbered as in Fig. 1.

except in this case the substrate was OPB (e.g., Buchs et al., 2010) as opposed to MORB or backarc basin crust. As in the case of Late Cretaceous Tethyan ophiolites and IBM forearc, there is no break between lower oceanic tholeiites and upper arc sequences (although more work is needed to test this for Caribbean PAR sequences). The PISI model for Late Cretaceous plume- and arc-related sequences provides a simple explanation for SI as well as the magmatic evolution, especially the apparent absence of a hiatus between lower CLIP and upper arc sequences. The principal difference with SI models for IBM and Tethyan ophiolites explored by Whattam and Stern (2011) is that the SW Caribbean Arc is built on plume-like sequences as opposed to MORB-like ones. These relations suggest that Late Cretaceous arrival of the Caribbean plume head triggered development of the Late Cretaceous arcs in Central America, Leeward Antilles, and NW South America. As expected, SI associated with near coeval plume-related magmatism imparted a plume 'flavor' on the earliest-formed South Caribbean plume- and arc-related unit lavas and intrusives as documented in Section 4. Apart from these plume-inherited characteristics, the Central American and NW South American plume- and arc-related units exhibit the same evolution as SI units of Tethyan-type ophiolites and intra-oceanic forearc crust, i.e., a progression to arc-like affinities with time. This difference in earliest SI magma chemistries may be key for discriminating between SI events triggered by plume (OIB- or OPB-like) from those not catalyzed by plume emplacement (MORB-like).

In Section 4 we demonstrated the overlapping trace element chemistry and isotopic composition of earlier and later plume- and arc-related units. We note here that overlapping trace element and particularly isotopic affinities between earliest circa 90–85 Ma underlying units interpreted as CLIP and younger, unambiguous arc-like products have been recognized for complexes in Panama (Buchs et al., 2010), Colombia (Kerr et al., 2004), Ecuador (Allibon et al., 2008), and the Leeward Antilles (White et al., 1999) which are consistent with substantial plume-subduction interactions. For example, on the basis of trace element chemistry, Buchs et al. (2010) note that proto-arc lavas and intrusives of the 75–66 Ma Golfito Complex (southern Costa Rica) are compositionally bracketed by CLIP and arc-like end-members. Using the circa 85–64 Ma Rio Cala Arc unit which was constructed atop the 90–85 Ma Pallatanga Unit (interpreted as CLIP) in Ecuador as another example, Nd and Pb isotopic compositions show that Rio Cala Arc lavas are consistent with mixing Pacific MORB-mantle, subducted pelagic sediments and an oceanic plateau component (Allibon et al., 2008). Another example of mixed plume-arc sources comes from circa 90–79 Ma Aruba Batholith subduction-related magmas which are isotopically similar to the underlying 103–89 Ma Aruba Lava Formation unit (interpreted as CLIP) they intrude (White et al., 1999). All of these observations are consistent with plume-subduction interactions and apart from the Golfito Complex, provide evidence for subduction initiation quickly following or accompanying plume emplacement.

5.4. Is there a hiatus between Late Cretaceous CLIP and arc igneous activity?

A key test of our SW Caribbean PISI model lies in understanding the transition between older plume-related CLIP units and younger, subduction-related arc sequences. Our Caribbean PISI model considers that subduction zones associated with Tr1–Tr3 formed in response to the Caribbean Plume and that the transition from plume to subduction happened while the plume was still active. In the cases of forearc-derived Tethyan ophiolites of the Mediterranean–Persian Gulf region and the Izu-Bonin forearc – all of which have been interpreted as forming in response to subduction initiation – there is a continuous transition upward from early MORB-like to younger arc-like sequences, without an appreciable break in the record (Reagan et al., 2010; Whattam and Stern, 2011; Stern et al., 2012). In the case of the Late Cretaceous evolution of the SW Caribbean, an important break in the stratigraphic record such as a major unconformity or an intervening sedimentary sequence would challenge the PISI model and support models that interpret older CLIP and younger arc sequences as forming in independent tectonic environments. In southern Panama, there exists an apparent ~10 Ma time gap between radiometric ages for the Early Sona–Azuero (89–85 Ma) 'plateau' and the Later Sona–Azuero proto-arc (initiated at 75–73 Ma; Buchs et al., 2010). The significance of this hiatus is unclear because no known unconformity or sedimentary package separates the two units, nor are the two units known to be fault-bounded. However, basalts of the Azuero Plateau record subduction additions and N-MORB signatures that overlap those of the younger Azuero Arc (at least one sample interpreted as Azuero Plateau also exhibits primitive-mantle normalized HFSE anomalies along with other lavas interpreted as plateau elsewhere; see the GR Online Supplementary Document). If the hiatus is real, it may support the idea that a significant change in tectonic environment occurred in the Late Cretaceous, calling for models entailing early plateau and later arc, at least in southern Panama. If the apparent hiatus is an artifact of inadequate radiometric ages then the PISI model is supported.

The apparent temporal gap for Panama is illustrated in Fig. 2, which also shows representative stratigraphic columns for other southern Caribbean PAR units documented in this study. Further field and geochronologic studies could resolve this question by testing the reality of the 10 Ma gap, for example by documenting a heretofore unrecognized interval of Late Cretaceous sedimentary rocks, hardground, or unconformity separating the youngest CLIP lavas and the oldest proto-arc lavas, or by obtaining more reliable radiometric ages targeted to locate the hiatus. We reiterate that more focused stratigraphic and radiometric studies are needed, but that until the presence of such a break is documented, we should consider further the PISI model for the Late Cretaceous tectonic evolution of the SW Caribbean region.

5.5. Critical evaluation of existing models for SW Caribbean subduction zone formation

5.5.1. Little evidence for collision-induced SI

An important consideration in deciding whether the Caribbean PISI model has merit is whether or not it answers more questions than existing models for SI in Tr1, Tr2, and Tr3. It is especially important to evaluate other models for why these subduction zones formed. Existing explanations for SI in Tr1, Tr2, and Tr3 rely on mechanisms of induced nucleation of subduction zone (INSZ; Stern, 2004). INSZ explanations identify collisions at one subduction zone as causing a new one to form. We show below that existing models for SI in the region of interest do not adequately explain how these traces formed.

The reason for Central American (Tr1) SI is controversial. The Greater Antilles Arc (GAA) was magmatically active beginning in the Early Cretaceous (perhaps as early as ~135 Ma; Pindell et al., 2011). Some tectonic models (e.g., Duncan and Hargraves, 1984; Pindell and Barrett, 1990; Hoernle et al., 2002; Mann, 2007) suggest that east-dipping subduction beneath Central America began after the CLIP jammed a NE-dipping subduction system beneath the GAA (see Fig. 4 of Hoernle et al., 2002). This interpretation was especially popular in early tectonic models but recent studies challenge this explanation. We are not convinced by the evidence supporting interpretation of an Early Cretaceous, NE-dipping subduction zone beneath the GAA. Lebron and Perfit (1993) argued that the mid-Cretaceous (~120–100 Ma) unconformity in Hispaniola and Puerto Rico could have reflected uplift accompanying CLIP-GAA collision, which led to a subduction polarity reversal, and that this unconformity also separated volcanic suites of distinct compositions (older arc tholeiites and younger calc-alkaline sequences; Lebron and Perfit, 1993). Jolly et al. (2008) agreed that Puerto Rico volcanic sequences were interrupted by mid-Cretaceous unconformities but noted that other Cretaceous arc successions in surrounding regions were conformable and concluded that the stratigraphic breaks were not due to collision. This interpretation is supported by the observation that mid-Cretaceous unconformities

are common all around the Pacific basin, perhaps due to superplume activity at this time (Vaughan, 1995). It appears that the subduction zone beneath the GAA dipped to the SW throughout its ~90 Ma lifespan, the same polarity that the subduction zone beneath the Lesser Antilles has today.

García-Casco et al. (2008) summarized evidence that the western GAA collided during latest Cretaceous–earliest Tertiary time with a thickened sedimentary pile they called "Caribeana" (see also Pindell et al., 2011). A similar interpretation comes from studies of GAA exposures in Hispaniola, with subduction continuing into the Eocene (Jolly et al., 2001). The timing of this event appears to be at least 10 Ma too late to have triggered Central American SI and there is no evidence to support a tectonic regime other than that of continuous SW dipping subduction beneath the GAA. We conclude that this "soft" collision did not trigger SI beneath Central America.

GAA arc volcanism continued until North America entered and jammed the S-dipping subduction zone beneath the GAA. This collision began as early as 70–60 Ma (Lázaro et al., 2009) and continued until ~40 Ma (Iturralde-Vinent et al., 2008). The long-lived nature of the GAA is also reflected in the >70 Ma history of arc volcanism documented in Puerto Rico, from ~120 to ~45 Ma (Jolly et al., 2001). Terminal collision between the Cuban segment of the GAA and North America also occurred in the Paleogene (Iturralde-Vinent et al., 2008; van Hinsbergen et al., 2009), with arc volcanism continuing up to ~62 Ma (Rojas-Agramonet et al., 2011). We conclude that subduction continued beneath parts of the GAA until ~45 Ma, significantly later than the beginning of subduction beneath Central America in the Late Cretaceous. For this reason, GAA-North America collision is also unlikely to have triggered Central America SI. The observation that collisions on the other side of the Caribbean plate either did not occur, were too "soft", or were too young to have induced Tr1 subduction favors a non-collisional induced SI model.

5.5.2. Necessity of west-dipping subduction to facilitate eastwards emplacement of PAR units upon South America

A fundamental assumption in many tectonic models for the Late Cretaceous evolution of the southern Caribbean and NW South America realm posit 'obduction' of plateau to the east above an east-dipping subduction zone beneath NW South America (e.g., Kerr et al., 1999; Hastie and Kerr, 2010; Hastie et al., 2013). However, this is mechanically implausible as obduction must occur in a direction opposing subduction zone dip; if subduction was to the east then obduction would be to the west which would have emplaced NW South America upon the plateau (i.e., the plateau would have been subducted, at least partially, eastwards beneath South America). Eastward obduction of CLIP units upon South America requires a W-dipping subduction zone as illustrated by Vallejo et al. (2009; see their Fig. 10). Original east-dipping subduction requires a subduction flip above which western Colombian and western Ecuadorian plume- and arc related units were emplaced, but there is no evidence for such a polarity reversal as discussed above. Furthermore, a subduction zone polarity flip would be expected to lead to a magmatic gap during the tectonic reconfiguration and a discernible change in chemistry between initial plume-only assemblages and post-flip subduction-modified assemblages. However this is not what we see in western Ecuadorian and Colombian plume- and arc-related units but instead an uninterrupted interval of post-100 Ma hybrid subduction-plume magmatism which records – albeit somewhat erratic – increases in Ba/Th, Ba/Nb and Th/Nb with time (Figs. 8–10).

West-dipping subduction in the vicinity of NW South America is required in any tectonic model regardless of the mode of SI as eastward emplacement requires westward subduction. West-dipping subduction is also a requirement of our PISI model (Figs. 14, 15) because original subduction vectors at any point along the periphery of the ~100 Ma plume would necessarily have been directed toward the center of the plume (Fig. 13a) (Burov and Cloetingh, 2010). Rapid retreat of the slab

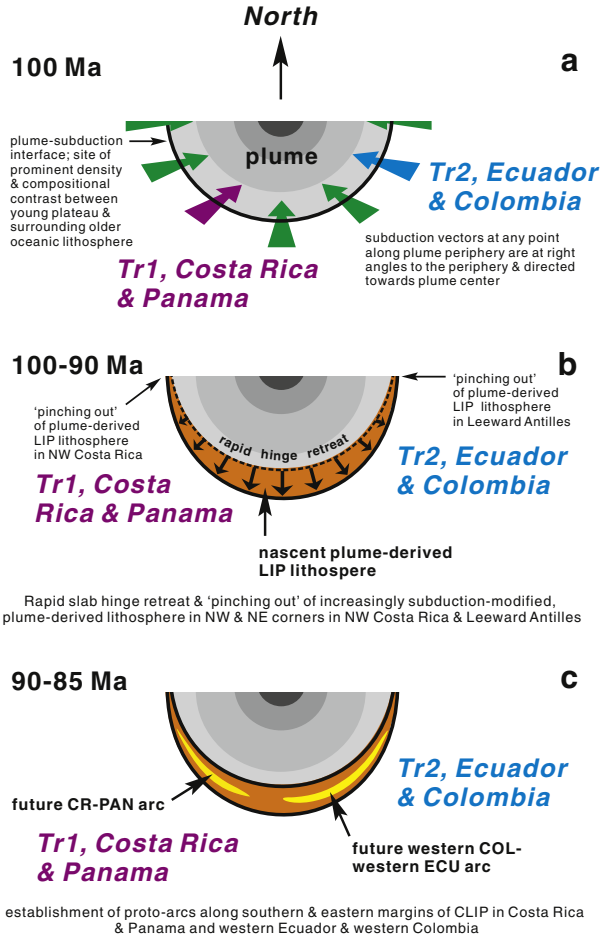

Fig. 13. Plan cartoon depiction of (a) initial PISI at 100 Ma, (b) rapid slab hinge rollback at 100–90 Ma and (c) establishment of arc construction at 90–85 Ma along the southern and eastern margins of the CLIP in Tr1 in Costa Rica and Panama and in Tr2 in western Ecuador and western Colombia. See text for details.

hinge and the 'pinching out' of PISI-derived lithosphere at the NW and NE corners of the LIP-subduction interface (Fig. 13b) may explain the termination of the PISI-derived lithosphere in NW Costa Rica and the Leeward Antilles. Further discussion on the necessity of west-dipping subduction to facilitate emplacement of SW South American PAR units is provided in the GR Online Supplementary Document.

5.6. Advantages of a PISI model for understanding Caribbean tectonic evolution

On the basis of geochemical, geochronological and tectonic constraints we infer that the Late Cretaceous tectono-magmatic evolution of southern Central America and NW South America was characterized by an episode of spontaneous nucleation of subduction along the periphery of a plume that was emplaced ~100 Ma (Fig. 14a–e; tectonic reconstructions are provided in Fig. 14f–j). Our "SW Caribbean PISI model" builds on geodynamic models presented by Ueda et al. (2008) and Burov and Cloetingh (2010). The principal way that the SW Caribbean PISI model differs from their models is that SI occurred only on one side of the plume (Fig. 15), not symmetrically all around the CLIP. This is not surprising, because subduction beneath the NE margin to form the GAA occurred some tens of Ma before SI on the three SW Caribbean traces began. The Caribbean Plume event may have been some sort of backarc basin magmatism associated with the GAA, but it is not necessary for the PISI model that the precise nature of the plume event be understood, only that sufficiently dense lithosphere was adjacent to a large enough plume such that plume emplacement

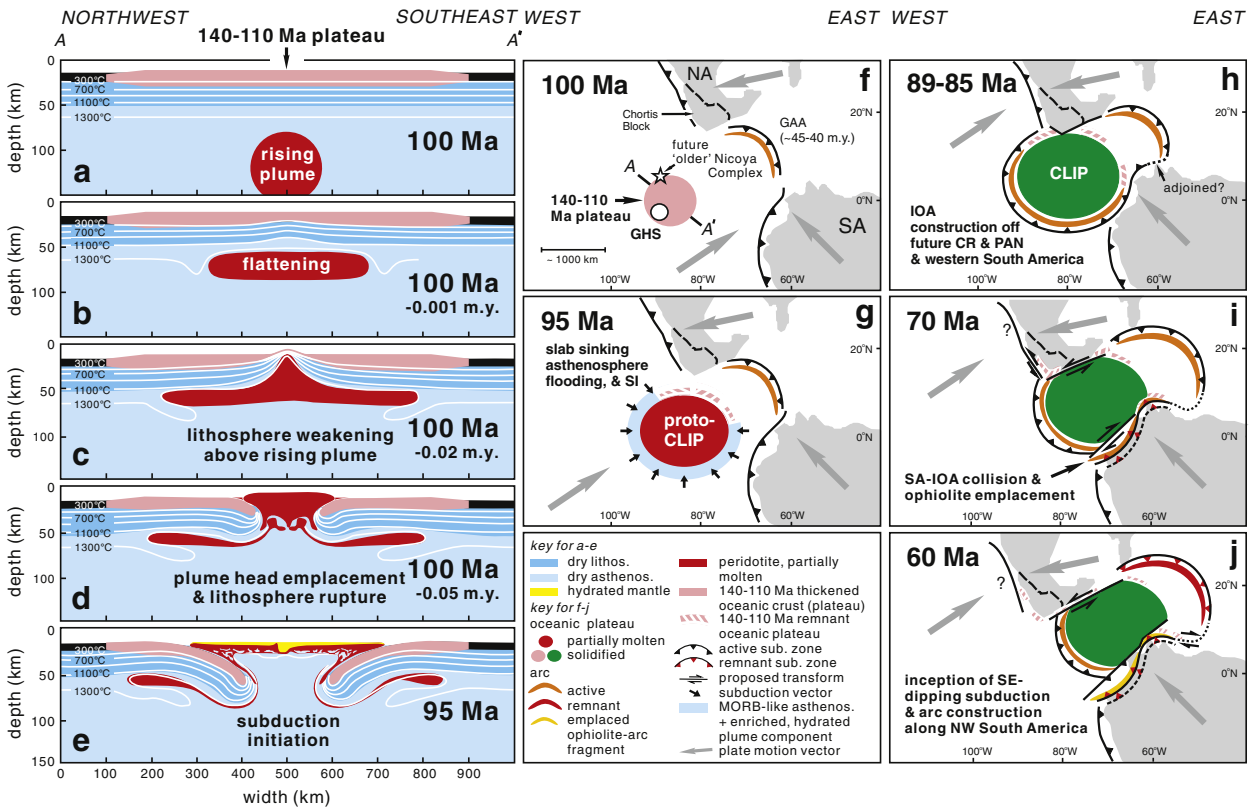

Fig. 14. PISI model (a-e) and 100-60 Ma tectonic reconstructions (f-j). PISI model is based on and modified from Ueda et al. (2008). A (west) and A' (east) for (a–e) is shown in (f). In (a), the (b) plume rises to the lithosphere base and flattens. (c) A central plume wedge rises and weakens the surrounding lithosphere. (d) The partially molten plume head ruptures the lithosphere and begins to spread. (e) Subduction initiates in response to plume emplacement. (f) The Farallon Plate comprised a segment of circa 140–100 Ma thickened oceanic crust represented at least in part, by the 140–110 Ma segment of the Nicoya Complex, western Costa Rica (see text); this older thickened oceanic crust was likely the substrate upon which the volumetrically dominant, post-100 Ma CLIP was constructed. As depicted in (e), emplacement of the mantle plume possibly above the Galapagos hotspot (GHS) (f) instigates (g) lithosphere sinking, subsequent asthenospheric flooding and ultimately SI. (h) SI results in arc construction along Costa Rica and Panama, western South America in Ecuador and Colombia and the Leeward Antilles (Aruba and Curaçao) (PISI traces 1–3, Fig. 1). (i) Collision of South America with the arc system off of western South America at ~ 70 Ma results in emplacement of intra-oceanic arc (IOA) ophiolitic fragments (dark yellow) in Colombia and Ecuador (see text for details). (j) E/SE dipping subduction nucleates to the west of South America. M.y. = millions of years.

caused a lithospheric weakness (Fig. 15b) that allowed flanking dense lithosphere to flex downward (Fig. 15c). It was not coincidental that SI immediately followed plume head emplacement but rather that SI was catalyzed by the plume head. As terminal magmatism of the 140–110 Ma plateau occurred ~10 Ma prior to the start of post-100 Ma CLIP magmatism, we suggest that pre-existing compositional and density contrasts between the 140–110 Ma plateau and its surrounding 'normal' oceanic lithosphere (Niu et al., 2003) created a favorable site for subduction to subsequently nucleate upon younger plateau extrusion beginning at 100 Ma.

Because it is the dense lithosphere adjacent to the plume that sinks to form a subduction zone, the PISI model predicts that subduction zones will dip beneath and toward the center of the plume as explained above (Burov and Cloetingh, 2010; and as shown in Fig. 13a). For Tr1, the Central American subduction zone has dipped continuously eastward since it formed in the Late Cretaceous. The subduction zone beneath Tr3 also resulted in a subduction zone that dipped northward, beneath the CLIP plume. This would have quickly brought northern South America into this subduction zone, jamming it and shutting it down by ~73 Ma as observed. The original dip of the subduction zone beneath Tr2 is not easily constrained, but the presence of former E-dipping subduction zones along the Pacific margin of South America may have influenced its development.

The recognition of increasing subduction additions and degrees of partial melting and overlapping isotopic composition between post-100 Ma plume and arc in the oldest sequences interpreted as CLIP are key arguments for our PISI model. As the rising plume-head arrived at the base of the lithosphere, the latter was weakened via heating, pervasive melt infiltration (Ueda et al., 2008) and diking. Lithosphere above the plume became more buoyant as flood basalts thickened the crust and heating thinned the mantle root (Laske et al., 2007), while oceanic lithosphere beyond the plume-affected (rejuvenated) region remained cold and dense. The lithospheric transition between rejuvenated and unaffected lithosphere localized differential vertical motions between buoyant and dense lithosphere (Fig. 15b). This lithospheric transition would have been arcuate in map view, centered on the plume axis. Dense lithosphere near this transition was able to flex downward around the plume margins (Fig. 15c). Sinking of old lithosphere may have been enhanced as plume-related lavas buried parts of the old seafloor (Fig. 14g). Downward-flexing lithosphere ultimately sank deep enough that motion changed from vertical to edge-on and this marked when the new subduction zones formed, with attendant development of arc magmatic systems around the nascent LIP margins (Fig. 13c). The magmatic progression of this plume-arc evolution is preserved in the rock record from Tr1–Tr3 that we have studied.

Our interpretation of the Late Cretaceous tectono-magmatic evolution of this region is consistent with numerical geodynamic experiments (Ueda et al., 2008; Burov and Cloetingh, 2010) and explains systematic temporal changes in magma compositions outlined above, at the same time reconciling many of the inconsistencies and difficulties of current tectonic models for the region. PISI is also consistent with the geochemistry and isotopic composition of many units which are intermediate between "plume" and "arc" affinities and similar in some respects to nascent SI units. Our PISI model is also consistent with the lack of evidence for any hiatus separating the 'CLIP' basement fragments

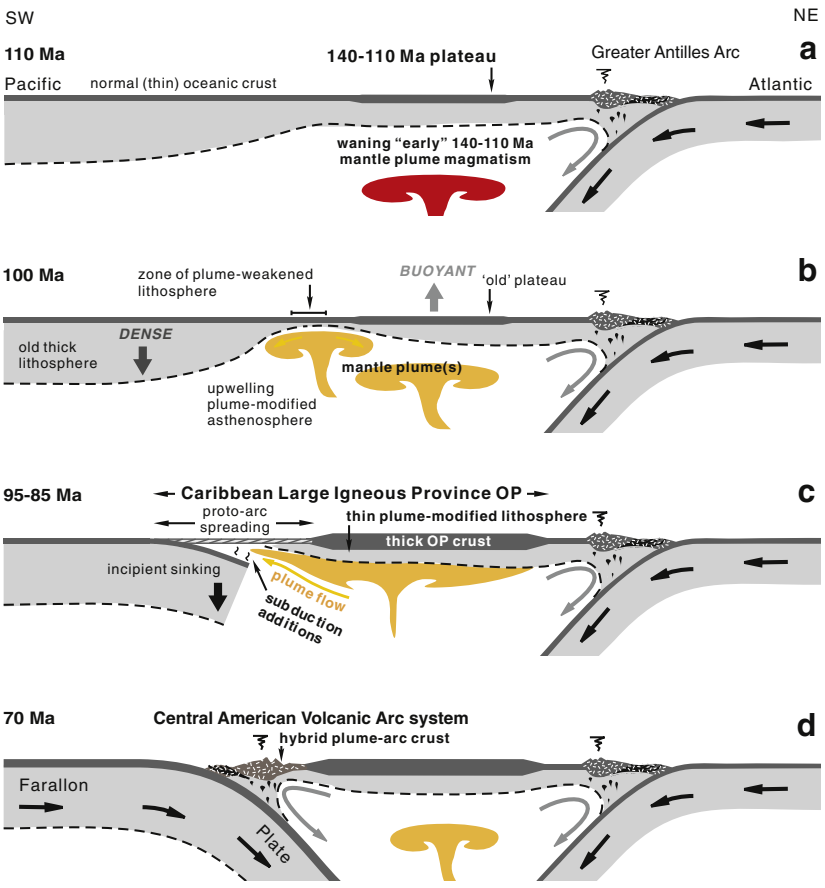

Fig. 15. Cartoon depicting construction of (a) the early 140–110 Ma oceanic plateau followed by the subsequent evolution of PISI between (b) 100 Ma, (c) 95–85 Ma and (d) 70 Ma.

in Panama and western Ecuador from the overlying arc units (e.g., Vallejo et al., 2009; Buchs et al., 2010; see also Fig. 2).

We recognize that a circum-CLIP subduction zone, or its fossil remainder, must have undergone considerable shape transformation/passive deformation to arrive at the present configuration shown in Fig. 1: a semi-circular, U-shape, has transformed, likely via a V-shape, into a Y-shape (Tr1 = left arm, Tr3 = right arm, and Tr2 = vertical). The details of how and when this complex oroclinal bending was accomplished are not clear, but interactions with NW South America must be key. Understanding this reconfiguration will require more work and is beyond the scope of our study.

5.7. Implications of the PISI model for understanding how plate tectonics began

Confirmation of the PISI model provides important new insights into Earth's tectonic evolution. As plate tectonics must have been begun without the sorts of plate tectonic-induced lithospheric weakness that are today called for in most SI models, articulation of the Caribbean PISI example helps us understand how the first subduction zones required to start global plate tectonics began. Because most of the force driving plate motions today results from the sinking of dense lithosphere in subduction zones (Lithgow-Bertelloni and Richards, 1995), the question of how plate tectonics began must focus on understanding how the first subduction zone formed. The key to understanding this is knowing what caused lithospheric weakness of sufficient extent (hundreds to 1000s of kilometers long) along which oceanic lithosphere could collapse. One possibility is large meteorite impact (Hansen, 2007), but impacts sufficiently large to weaken a large enough region of the lithosphere may only have occurred in Hadean times, when lithosphere was probably not dense enough and strong enough to subduct. Bercovici and Ricard (2014) recently suggested that lithospheric damage – perhaps resulting from delamination – promoted shear localization and weak zones. They argued that this lithospheric fabric combined with transient mantle flow to form the first subduction zone and plate tectonics, but it is not clear that lithospheric weak zones would be weak enough and long enough to allow lithosphere to sag and sink beneath underlying asthenosphere. Another possibility is plume-induced subduction initiation (PISI) whereby a mantle plume head (or other large-scale asthenospheric upwelling) weakened the lithosphere when it impinged on its base. Lithosphere weakening results from thermal effects and dike injection (Burov et al., 2007). PISI may have been more important in Precambrian times than it is today, because plume heads were likely hotter and larger and lithosphere was thinner and weaker. The Caribbean PISI example suggests that the modern plate tectonics regime became effective when early subduction zones formed as a lithospheric response to mantle upwelling similar to what we have described for the Late Cretaceous tectonic evolution of the SW Caribbean. Once early subduction zones were established and the horizontal translation of lithospheric plates was initiated, transform faults and other kinds of lithospheric weaknesses could be generated allowing for more subduction zones to form. We should consider seriously that interaction of a sufficiently large plume head with sufficiently dense oceanic lithosphere may have triggered the modern episode of plate tectonics.

6. Conclusions

On the basis of geochemical, isotopic, geochronological, stratigraphic and tectonic considerations we infer that the principal catalyst for forming subduction zones around the southern margin of the Caribbean

Plate and NW South America in the Late Cretaceous was the arrival of a mantle plume head circa 100 Ma which fed the near simultaneous eruption of the CLIP. Three fundamental observations support this conclusion: (1) There exists two geochemically and temporally distinct plateaus that were generated at 140–110 Ma and after 100 Ma. Distinct compositional differences exist between post-100 Ma units exposed along Tr1 and Tr2 (southern periphery of the Caribbean Plate and NW South America) and (i) the older plateau; and (ii) units in the center and northerly sections of the CLIP. Lavas and intrusives of the younger units exposed in Tr1 and Tr2 record evidence of subduction additions which increased with time beginning ~100 Ma; conversely, the older 140–110 Ma plateau and the post-100 Ma units in the northern and central regions of the CLIP record no evidence of subduction modification. (2) There are no obvious or documented breaks between post-100 Ma plume-related igneous sequences (CLIP) and overlying arc units. (3) Generation of the CLIP and earliest, overlying arc units overlap in time, space and trace element chemical and isotopic compositions. Compositions of the CLIP and arc units are both consistent with derivation from mantle associated with the Galapagos Plume which became increasingly subduction-modified with time beginning at 100 Ma.

This is the first convincing example of plume-induced subduction initiation, and the validation of this model opens doors for many avenues of further research, ranging from the need for more detailed studies of circum-Caribbean igneous suites to investigating why some mantle plumes evolve into subduction zones and others do not. We emphasize that many aspects of this model require further testing. For example, did the pre-existing subduction regime further south in South America and along the NE margin of the Caribbean plate contribute to PISI in the SW Caribbean? Perhaps this explains why Caribbean plume emplacement triggered SI around the Caribbean but not along other oceanic plateaus (e.g., the Ontong Java Plateau). Another important question is whether our interpretation of the Late Cretaceous tectonic development of this complex region advances understanding of how other subduction zones originated. If the PISI model is valid, it is unlikely that it only applies for the Caribbean plume-arc system and there should be other episodes of plume-induced subduction initiation. PISI may be useful for understanding how the modern Cascadia subduction zone formed which has been interpreted as forming in response to the arrival of the Yellowstone mantle plume in the Eocene (Wells et al., 1984). Another PISI candidate can be found in the Neoproterozoic of South China, where there is vibrant controversy as to whether 825–720 Ma igneous rocks formed in a mantle plume/rift setting or collision/arc setting (Wang et al., 2009). Finally, confirmation of the PISI model provides important new insights into Earth's tectonic evolution. PISI may have been more important in Precambrian times than it is today, because plume heads were likely hotter and larger and lithosphere was thinner and weaker. The Caribbean PISI example suggests that the modern-day plate tectonics regime may have begun when early subduction zones formed in response to arrival of a mantle plume head at the base of old, dense oceanic lithosphere. Establishment of early subduction zones and horizontal translation of lithospheric plates generated lithospheric weaknesses; subsequently, the proliferation of subduction zones heralded the onset of the modern plate tectonics regime.

Acknowledgments

We wish to thank T. Gerya for his positive comments on an earlier version of this manuscript and his invitation to submit this manuscript to Gondwana Research. K. Ueda and an anonymous reviewer are gratefully acknowledged for their meticulous, detailed and constructive reviews which greatly improved this paper. SAW acknowledges the financial support from the Smithsonian Tropical Research Institute in Panama City, Panama during his tenure there in 2010–2011. This is a UTD Geosciences contribution #1261.

Appendix A. Supplementary data

Supplementary data to this article can be found online at http://dx.doi.org/10.1016/j.gr.2014.07.011.

References

Allibon, J., Monjoie, P., Lapierre, H., Jaillard, E., Bussy, F., Bosch, D., Senebier, F., 2008. The contribution of the young Cretaceous Caribbean Oceanic Plateau to the genesis of late Cretaceous arc magmatism in the Cordillera Occidental of Ecuador. Journal of South American Earth Sciences 26, 355–368.
Alvarado, G.E., Denyer, P., Sinton, C.W., 1997. The 89 Ma Tortugal komatiitic suite, Costa Rica: implications for a common geological origin of the Caribbean and Eastern Pacific region from a mantle plume. Geology 25, 439–442.
Arculus, R.J., 2003. Use and abuse of the terms calcalkaline and calcalkalic. Journal of Petrology 44, 929–935.
Arndt, N.T., Kerr, A.C., Tarney, J., 1997. Dynamic melting in plume heads: the formation of Gorgona komatiites and basalts. Earth and Planetary Science Letters 146, 289–301.
Bandini, A.N., Flores, K., Baumgartner, P.O., Jackett, S.-J., Denyer, P., 2008. Late Cretaceous and Paleogene radiolaria from the Nicoya Peninsula, Costa Rica: a tectonostratigraphic application. Stratigraphy 5, 3–21.
Barbarin, B., 1999. A review of the relationships between granitoid types, their origins and their geodynamic environments. Lithos 46, 605–626.
Barrero, D., 1979. Geology of the Central Western Cordillera, west of Buga and Roldanillo, Colombia. Publicaciones Geologicas Especials del INGEOMINAS 4, 1–75.
Baumgartner, P.O., Flores, K., Bandini, A., Girault, F., Cruz, D., 2008. Upper Triassic to Cretaceous radiolaria from Nicaragua and northern Costa Rica—The Mesquito composite oceanic terrane. Ofioliti 33, 1–19.
Bercovici, D., Ricard, Y., 2014. Plate tectonics, damage, and inheritance. Nature 508, 513–516.
Bourgois, J., Toussaint, J.F., Gonzales, H., Azema, J., Calle, B., Desmet, A., Murcia, L.S., Acevedo, A.P., Parra, E., Tournon, J., 1987. Geological history of the Cretaceous ophiolitic complexes of NW South America (Colombian Andes). Tectonophysics 143, 307–327.
Beaudon, E., Martelat, J.E., Amortegui, A., Lapierre, H., Jaillard, E., 2005. Metabasites de la cordillere occidentale d'Equateur, temoins du soubassement oceanique des Andes 'Equateur. Comptes Rendus Geoscience 337, 625–634. http://dx.doi.org/10.1016/j.crte.2005.01.002.
Boland, M.L., Pilatasig, L.F., Ibadango, C.E., McCourt, W.J., Aspden, J.A., Hughes, R.A., Beate, B., 2000. Geology of the Cordillera Occidental of Ecuador between 0° and 1° N. Proyecto de Desarrollo Minero y Control Ambiental, programa de Informacion Cartografica y Geológica, CODIGEM-BGS, Quito, Informe. 10.
Bowland, C.L., Rosencrantz, E., 1988. Upper crustal structure of the western Colombian Basin, Caribbean Sea. Geological Society of America Bulletin 100, 534–546.
Brown, G.C., Thorpe, R.S., Webb, P.C., 1984. The geochemical characteritics of granitoids in contrasting arcs and comments on magma sources. Journal of the Geological Society of London 141, 413–426.
Buchs, D.M., Arculus, R.J., Baumgartner, P.O., Baumgartner-Mora, C., Ulianov, A., 2010. Late Cretaceous arc development on the SW margin of the Caribbean Plate: insights from the Golfito, Costa Rica, and Azuero, Panama, complexes. Geochemistry, Geophysics, Geosystems 11. http://dx.doi.org/10.1029/2009GC002901.
Buchs, D.M., Baumgartner, P.O., Baumgartner-Mora, C., Bandini, A.N., Jackett, S.-J., Diserens, M.-O., Stucki, J., 2009. Late Cretaceous to Miocene seamount accretion and mélange formation in the Osa and Burica peninsulas (southern Costa Rica): Episodic growth of a convergent margin. In: James, K.H., Lorente, M.A., Pindell, J.L. (Eds.), The Origin and Evolution of the Caribbean Plate. Geological Society (London) Special Publication. 328, pp. 411–456.
Burov, E., Cloetingh, S., 2010. Plume-like upper mantle instabilities drive subduction initiation. Geophysical Research Letters 37, L03309. http://dx.doi.org/10.1029/2009GL041535.
Burov, E., Guillou-Frottier, L., d'Acremonte, E., Le Pourhiet, L., Cloetingh, S., 2007. Plume head-lithosphere interactions near intra-continental plate boundaries. Tectonophysics 434, 15–38.
Canil, D., 1997. Vanadium partitioning and the oxidation state of Archaean komatiite magmas. Nature 389, 842–845.
Casey, J.F., Dewey, J.F., 1984. Initiation of subduction zones along transform and accreting boundaries, triple junction evolution, and forearc spreading centers—implications for ophiolite geology and obduction. In: Gass, I., Lippard, S.J., Shelton, A.W. (Eds.), Ophiolites and oceanic lithosphere. Geological Society of London Special Publication. 13, pp. 269–290.
Chiaradia, M., 2009. Adakite-like magmas from fractional crystallization and melting-assimilation of mafic lower crust (Eocene Macuchi arc, Western Cordillera, Ecuador). Chemical Geology 265, 468–487.
Cloos, M., 1993. Lithospheric buoyancy and collisional orogenesis: subduction of oceanic plateaus, continental margins, island arcs, spreading ridges and seamounts. Geological Society of America Bulletin 105, 715–737.
Cooper, P., Taylor, B., 1985. Polarity reversal in the Solomon Islands. Nature 314, 428–430.
Condie, K.C., Abbott, D.H., 1999. Oceanic plateaus and hotspot islands: identification and role in continental growth. Lithos 46, 1–4.
DeBari, S.M., Taylor, B., Spencer, K., Fujioka, K., 1999. A trapped Philippine Sea plate origin for MORB from the inner slope of the Izu-Bonin Trench. Earth and Planetary Science Letters 174, 183–197. http://dx.doi.org/10.1016/S0012-821X(99)00252-6./S0012-821X(99)00252-6.

DiMarco, G., Baumgartner, P.O., Channell, J.E.T., 1995. Late Cretaceous-early Tertiary paleomagnetic data and a revised tectonostratigraphic subdivision of Costa Rica and western Panama. In: Mann, P. (Ed.), Geologic and Tectonic Development of the Caribbean Plate Boundary in Southern Central America. Special Paper of the Geological Society of America. 295, pp. 1–27.
Donnelly, T.W., Melson, K., Kay, R., Rogers, J.J.W., 1973. Basalts and dolerites of Late Cretaceous age from the central Caribbean. In: Edgar, N.T., Saunders, J.B. (Eds.), Initial Reports of the Deep Seal Drilling Project. vol. 15. U.S. Government Printing Office, Washington, D.C., pp. 989–1012.
Drummond, M.S., Bordelon, M., de Boer, J.Z., Defant, M.J., Bellon, H., Feigenson, M.D., 1995. Igneous petrogenesis and tectonic setting of plutonic and volcanic rocks of the Cordillera de Talamanca, Costa Rica–Panama, Central American arc. American Journal of Science 295, 875–919.
Duncan, R.A., Hargraves, R.B., 1984. Plate tectonic evolution of the Caribbean region in the mantle reference frame. Geological Society of America Memoir 162, 81–93.
Dymkova, D., Gerya, T., 2013. Porous fluid flow enables oceanic subduction initiation on Earth. Geophysical Research Letters 40, 5671–5676.
Elliott, T., Plank, T., Zindler, A., White, W., Bourdon, B., 1997. Element transport from slab to volcanic front at the Mariana arc. Journal of Geophysical Research 102, 14,991–15,019.
Evans, K.A., Elburg, M.A., Kamenetsky, V.S., 2012. Oxidation state of subarc mantle. Geology 40, 783–786.
Frey, F.A., Weis, D., Yu. Borisova, A., Xu, G., 2002. Involvement of continental crust in the formation of the Cretaceous Kerguelen Plateau: new perspectives from ODP Leg 120 sites. Journal of Petrology 43, 1207–1239.
Frost, D.J., McCammon, C.A., 2008. The redox state of the Earth's mantle. Annual Review of Earth and Planetary Sciences 36, 389–420.
García-Casco, A., Iturralde-Vinent, M.A., Pindell, J., 2008. Latest Cretaceous collision/accretion between the Caribbean Plate and Caribeana: origin of metamorphic terranes in the Greater Antilles. International Geology Review 50, 781–809.
Gazel, E., Hoerle, K., Carr, M.J., Herzberg, C., Saginor, I., van den Bogaard, P., Hauff, F., Feigenson, M., Swisher III, C., 2011. Plume-subduction interaction in southern Central America: mantle upwelling and slab melting. Lithos 121, 117–134.
Gazel, E., Carr, M.J., Hoernle, K., Feigenson, M.D., Szymanski, D., Hauff, F., van den Bogaard, P., 2009. Galapagos-OIB signature in southern Central America: mantle refertilization by arc–hot spot interaction. Geochemistry, Geophysics, Geosystems 10, Q02S11. http://dx.doi.org/10.1029/2008GC002246.
Gurnis, M., Hall, C., Lavier, L., 2004. Evolving force balance during incipient subduction. Geochemistry, Geophysics, Geosystems 5, Q07001. http://dx.doi.org/10.1029/2003GC000681.
Hall, C., Gurnis, M., Sdrolias, M., Lavier, L.L., Müller, R.D., 2003. Catastrophic initiation of subduction following forced convergence across fracture zones. Earth and Planetary Science Letters 212, 15–30.
Hansen, V.L., 2007. Suduction origin on early Earth: a hypothesis. Earth and Planetary Science Letters 35, 1059–1062.
Hastie, A.R., Kerr, A.C., 2010. Mantle plume or slab window? Physical and geochemical constraints on the origin of the Caribbean oceanic plateau. Earth-Science Reviews 98, 283–293.
Hastie, A.R., Mitchell, S.F., Treloar, P.J., Kerr, A.C., Neill, I., Barfo, D.N., 2013. Geochemical components in a Cretaceous island arc: the Th/La–(Ce/Ce*)Nd diagram and implications for subduction initiation in the inter-American region. Lithos 162–163, 57–69.
Hauff, F., Hoernle, K., van der Bogard, P., 2000a. Age and geochemistry of basaltic complexes in western Costa Rica: contributions to the geotectonic evolution of Central America. Geochemistry, Geophysics, Geosystems 1 (Paper number 1999GC000020).
Hauff, F., Hoernle, K., Tilton, G., Graham, D.W., Kerr, A.C., 2000b. Large scale recycling of oceanic lithosphere over short time scales: geochemical constraints from the Caribbean Large Igneous Province. Earth and Planetary Science Letters 174, 247–263.
Hauff, F., Hoernle, K., Schmincke, H.-U., Werner, A., 1997. A Mid Cretaceous origin for the Galapagos hotspot: volcanological, petrological and geochemical evidence from Costa Rican oceanic crustal segments. Geologische Rundschau 86, 141–155.
Hoernle, K., Hauff, F., van den Bogaard, P., 2004. 70 m.y. history (139–69 Ma) for the Caribbean large igneous province. Geology 32, 697–700.
Hoernle, K., Hauff, F., van den Bogaard, P., Werner, R., Mortimer, N., Geldmacher, J., Garbe—Schönberg, D., Davy, B., 2010. Age and geochemistry of volcanic rocks from the Hikurangi and Manihiki oceanic plateaus. Geochimica et Cosmochimica Acta 74, 7196–7219.
Hoernle, K., van den Bogaard, P., Werner, R., Lissinna, B., Hauff, F., Alvarado, G., Garbe-Schonberg, D., 2002. Missing history (16–71 Ma) of the Galapagos hotspot: implications for the tectonic and biological evolution of the Americas. Geology 30, 795–798. http://dx.doi.org/10.1130/0091-7613.
Hughes, R., Bermúdez, R., 1997. Geology of the Cordillera Occidental of Ecuador between 0°00′ and 1° 00′S: Quito, Ecuador, Proyecto de Desarollo Minero y Control Ambiental. Programa de Información Cartográficay Geológica Report 4 (CODIGEM–British Geological Survey), (75 pp.).
Hughes, R.A., Pilatsig, L.F., 2002. Cretaceous and Tertiary terrane accretion in the Cordillera Occidental of the Andes of Ecuador. Tectonophysics 345, 29–48. http://dx.doi.org/10.1016/S0040-1951(01)00205-0.
Ingle, S., Mahoney, J.J., Sato, H., Coffin, M.F., Kimura, J.-I., Hirano, N., Nakanishi, N., 2007. Depleted mantle wedge and sediment fingerprint in unusual basalts from the Manihiki Plateau, central Pacific Ocean. Geology 35, 595–598.
Irvine, T.N., Baragar, W.R.A., 1971. A guide to the chemical classification of common volcanic rocks. Canadian Journal of Earth Sciences 8, 523–548.
Ishizuka, O., Tani, K., Reagan, M.K., Kanayama, K., Umino, S., Harigane, Y., Sakamoto, I., Miyajima, Y., Yuasa, M., Dunkley, D.J., 2011. The timescales of subduction initiation and subsequent evolution of an oceanic island arc. Earth and Planetary Science Letters 306, 229–240.
Iturralde-Vinent, M.A., Otero, C.D., García-Casco, A., Van Hinsbergen, D.J.J., 2008. Paleogene foredeep basin deposits of north-central Cuba: a record of arc-continent collision between the Caribbean and North American Plates. International Geology Review 50, 863–884.
Jaillard, E., Lapierre, H., Ordoñez, M., Álava, J.T., Amórtegui, A., Vanmelle, A., 2009. Accreted oceanic terranes in Ecuador: southern margin of the Caribbean Plate? Geological Society, London, Special Publications 328, 469–485.
Jaillard, E., Ordoñez, M., Benitez, S., Berrones, G., Jimenez, N., Montenegro, G., Zambrano, I., 1995. Basin development in an accretionary, oceanic-floored forearc setting: Southern coastal Ecuador during Late Cretaceous–late Eocene time. In: Tankard, A.J., Suárez Soruco, R., Welsink, H.J. (Eds.), Petroleum Basins of South America: American Association of Petroleum Geologists (AAPG) Memoir. 62, pp. 615–631.
Jolly, W.T., Lidiak, E.G., Dickin, A.P., Wu, T.-W., 2001. Secular geochemistry of Central Puerto Rican Island Arc lavas: constraints on Mesozoic tectonism in the Greater Antilles. Journal of Petrology 42, 2197–2214.
Jolly, W.T., Lidiak, E.G., Dickin, A.P., 2008. The case for persistent southwest-dipping Cretaceous convergence in the northeast Antilles: geochemistry, melting models, and tectonic implications. Geological Society of America Bulletin 120, 1036.
Jordan, E.K., Liu, W., Stern, R.J., Carr, M.J., Feigenson, M.D., Gill, J.B., Lenert, K., 2012. Geochemical Data Library for Quaternary Lavas of Lavas from the Magmatic Front of the Central America and Izu-Bonin Mariana Arc: Explanation to Accompany Excel Workbook CentAm & IBM Geochem Database version 1.02: MARGINS Subduction Factory Synthesis and Integration Project April 4, 2012.
Kemp, D.V., Stevenson, D.J., 1996. A tensile flexural model for the initiation of subduction. Geophysical Journal 125, 73–94.
Kessler, S.E., Sutter, J.F., Issigonis, M.J., Jones, L.M., Walker, R.L., 1977. Evolution of copper porphyry mineralization in an oceanic island arc: Panama. Economic Geology 72, 1142–1153.
Kerr, A.C., Iturralde-Vinent, M., Saunders, A.D., Babbs, T.L., Tarney, J., 1999. A new plate tectonic model of the Caribbean: implications from a reconnaissance of Cuban Mesozoic volcanic rocks. Geological Society of America Bulletin 111, 1581–1599. http://dx.doi.org/10.1130/0016-7606(1999)111<1581:ANPTMO>2.3.CO;2.
Kerr, A.C., Aspden, J.A., Tarney, J., Pilatsig, L.F., 2002a. The nature and provenance of accreted oceanic terranes in western Ecuador: geochemical and tectonic constraints. Journal of the Geological Society of London 159, 577–594. http://dx.doi.org/10.1144/0016-764901-151.
Kerr, A.C., Marriner, G.F., Arndt, N.T., Tarney, J., Nivia, A., Saunders, A.D., Duncan, R.A., 1996a. The petrogenesis of Gorgona komatiites, picrites and basalts: new field, petrographic and geochemical constraints. Lithos 37, 245–260.
Kerr, A.C., Marriner, G.F., Tarney, J., Nivia, A., Saunders, A.D., Thirlwall, M.J., Sinton, C.W., 1997. Cretaceous basaltic terranes in western Colombia: elemental, chronological and Sr–Nd isotopic constraints on petrogenesis. Journal of Petrology 38, 677–702.
Kerr, A.C., Pearson, D.G., Nowell, G.M., 2009. Magma source evolution beneath the Caribbean oceanic plateau: new insights from elemental and Sr–Nd–Pb–Hf isotopic studies of ODP Leg 165 Site 1001 basalts. In: James, K.H., Lorente, M.A., Pindell, J.L. (Eds.), The Origin and Evolution of the Caribbean Plate. Geological Society of London Special Publications. 328, pp. 809–827.
Kerr, A.C., Tarney, J., Kempton, P.D., Pringle, M., Nivia, I., 2004. Mafic pegmatites intruding oceanic plateau gabbros and ultramafic cumulates from Bolívar, Colombia: evidence for a 'wet' mantle plume? Journal of Petrology 45, 1877–1906.
Kerr, A.C., Tarney, J., Marriner, G.F., Klaver, G.T., Saunders, A.D., Thirlwall, M.F., 1996b. The geochemistry and petrogenesis of the Late-Cretaceous picrites and basalts of Curacao, Netherlands Antilles: a remnant of an oceanic plateau. Contributions to Mineralogy and Petrology 124, 29–43.
Kerr, A.C., Tarney, J., Kempton, P.D., Spadea, P., Nivia, A., Marriner, G.F., Duncan, R.A., 2002b. Pervasive mantle plume head heterogeneity: Evidence from the late Cretaceous Caribbean–Colombian Oceanic Plateau. Journal of Geophysical Research 107. http://dx.doi.org/10.1019/2001JB000790.
Kerr, A.C., White, R.V., Thompson, P.M., Tarnez, J., Saunders, A.D., 2003. In: Bartolini, C., Buffler, R.T., Blickwede, J. (Eds.), The Circum-Gulf of Mexico and the Caribbean: hydrocarbon habitats, basin formation, and plate tectonics: American Association of Petroleum Geologists (AAPG) Memoir. 79, pp. 126–188.
Kerr, A.C., White, R.V., Saunders, A.D., 2000. LIP reading: recognizing oceanic plateaux in the geological record. Journal of Petrology 41, 1041–1056.
Kolarsky, R.A., Mann, P., Monechi, S., Meyerhoff, H.D., Pessagno Jr., E.A., 1995. Stratigraphic development of southwestern Panama as determined from integration of marine seismic data and onshore geology. In: Mann, P. (Ed.), Geologic and Tectonic Development of the Caribbean Plate Boundary in Southern Central America. Special Paper of the Geological Society of America. 295, pp. 159–200.
Korenaga, J., 2013. Initiation and evolution of plate tectonics on Earth: theory and observations. Annual Review of Earth and Planetary Sciences 41, 117–151.
Kuno, H., 1968. Differentiation of basalt magmas. In: Hess, H.H., Poldervaart, A.A. (Eds.), Basalts: The Poldervaart Treatise on Rocks of Basaltic Composition, 2. Interscience, New York, pp. 623–688.
Lapierre, H., Bosch, D., Dupuis, V., Polve, M., Maury, R., Hernandez, J., Monie, P., Yeghicheyan, D., Jaillard, E., Tardy, M., Mercier de Lepinay, B., Mamberti, M., Desmet, A., Keller, F., Senebier, F., 2000. Multiple plume events in the genesis of the peri-Caribbean Cretaceous oceanic plateau province. Journal of Geophysical Research 105, 8403–8421. http://dx.doi.org/10.1029/1998JB900091.
Lapierre, H., Dupuis, V., de Lépinay, B.M., Bosch, D., Monié, P., Tardy, M., Maury, R.C., Hernandez, J., Polvé, Yeghicheyan, D., Cotten, J., 1999. Late Jurassic oceanic crust

and Upper Cretaceous Caribbean Plateau picritic basalts exposed in the Duarte Igneous Complex, Hispaniola. Journal of Geology 107, 193–207.
Lapierre, H., Dupuis, V., de Lépinay, B.M., Tardy, M., Ruíz, J., Maury, R.C., Hernandez, J., Loubet, M., 1997. Is the Lower Duarte Igneous Complex (Hispaniola) a remnant of the Caribbean plume-generated oceanic plateau? Journal of Geology 105, 111–120.
Laske, G., Phipps Morgan, J., Orcutt, J.A., 2007. The Hawaiian SWELL pilot experiment—Evidence for lithosphere rejuvenation from ocean bottom surface wave data. In: Foulger, G.R., Jurdy, D.M. (Eds.), Plates, plumes, and planetary processes. Geological Society of America Special Paper. 430, pp. 209–233.
Lázaro, C., García-Casco, A., Rojas Agramonte, Y., Kröner, A., Neubauer, F., Iturralde-Vinent, M., 2009. Fifty-five- million-year history of oceanic subduction and exhumation at the northern edge of the Caribbean plate (Sierra del Convento mélange, Cuba). Journal of Metamorphic Geology 27, 19–40.
Lebron, M.C., Perfit, M.R., 1993. Stratigraphic and petrochemical data support subduction polarity reversal of the Caribbean Island Arc. Journal of Geology 101, 389–396.
Lissinna, B., 2005. A profile through the Central American Landbridge in western Panama: 115 Ma interplay between the Galápagos Hotspot and the Central American Subduction Zone. (Ph.D. thesis) Christian-Albrechts University, Kiel, Germany, (102 pp.).
Lithgow-Bertelloni, C., Richards, M.A., 1995. Cenozoic plate driving forces. Geophysical Research Letters 22, 1317–1320.
Loewen, M.W., Duncan, R.A., Kent, A.J.R., Krawl, K., 2013. Prolonged plume volcanism in the Caribbean Large Igneous Province: new insights from Curacao and Haiti. Geochemistry, Geophysics, Geosystems 14. http://dx.doi.org/10.1002/ggge.20273.
Luzieux, L.D.A., Heller, F., Spikings, F., Vallejo, C.F., Winkler, W., 2006. Origin and Cretaceous tectonic history of the coastal Ecuadorian forearc between 1°N and 3°S: paleomagnetic, radiometric and fossil evidence. Earth and Planetary Science Letters 249, 400–414. http://dx.doi.org/10.1016/j.epsl.2006.07.008.
MacDonald, W.D., 1968. Communication. Status of geological research in the Caribbean. 14. University of Puerto Rico, p. 40.
Mahoney, J.J., Jones, W.B., Frey, F.A., Salters, V.J.M., Pyle, D.G., Davies, H.L., 1995. Geochemical characteristics of lavas from Broken Ridge, the Naturaliste Plateau and southernmost Kerguelen Plateau: early volcanism of the Kerguelen hotspot. Chemical Geology 120, 315–345.
Mahoney, J.J., Storey, M., Duncan, R.A., Spencer, K.J., Pringle, M., 1993. Geochemistry and geochronology of the Ontong Java Plateau. In: Pringle, M., Sager, W., Sliter, W., Stein, S. (Eds.), The Mesozoic Pacific: Geology, Tectonics, and Volcanism: Geophysical Monograph 77. American Geophysical Union, pp. 233–261.
Mamberti, M., Lapierre, H., Bosch, D., Jaillard, E., Ethiene, R., Hernandez, J., Polvé, M., 2003. Accreted fragments of the Late Cretaceous Caribbean–Colombian Plateau in Ecuador. Lithos 66, 173–199.
Mamberti, M., Lapierre, H., Bosch, D., Jaillard, E., Hernandez, J., Polvé, M., 2004. The Early Cretaceous San Juan Plutonic suite, Ecuador: a magma chamber in an oceanic plateau? Canadian Journal of Earth Sciences 41, 1237–1258.
Mann, P., 2007. Overview of the tectonic history of northern Central America. In: Mann, P. (Ed.), Geologic and tectonic development of the Caribbean plate boundary in northern Central America. Geological Society of America Special Paper. 428, pp. 1–19.
Mart, Y., Aharonov, E., Mulugeta, G., Ryan, W., Tentler, T., Goren, L., 2005. Analogue modelling of the initiation of subduction. Geophysical Journal International 160, 1081–1091.
McKenzie, D.P., 1977. The initiation of trenches: a finite amplitude instability. In: Talwani, M., Pitman III, W.C. (Eds.), Island arcs, deep sea trenches and back-arc basins. American Geophysical Union, Maurice Ewing Series. 1, pp. 57–61.
Miyashiro, A., 1974. Volcanic rock series in island arcs and active continental margins. American Journal of Science 274, 321–355.
Montes, C., Bayona, G., Cardona, A., Buchs, D.M., Silva, C.A., Morón, S., Hoyos, N., Ramírez, D.A., Jaramillo, C.A., Valencia, V., 2012. Arc–continent collision and orocline formation: closing of the Central American seaway. Journal of Geophysical Research 117. http://dx.doi.org/10.1029/2011JB008959.
Neal, C.R., Mahoney, J.J., Chazey, W.I., 2002. Mantle sources and the highly variable role of continental lithosphere in basalt petrogeneisis of the Kerguelen Plateau and the Broken Ridge LIP: results from ODP Leg 193. Journal of Petrology 43, 1177–1205.
Nikolaeva, K., Gerya, T.V., Marques, F.O., 2010. Subduction initiation at passive margins: numerical modeling. Journal of Geophysical Research 115, B03406. http://dx.doi.org/10.1029/2009JB006549.
Niu, Y., O'Hara, M.J., Pearce, J., 2003. Initiation of subduction zones as a consequence of lateral compositional buoyancy contrast within the lithosphere: a petrological perspective. Journal of Petrology 44, 851–866. http://dx.doi.org/10.1093/petrology/44.5.851.
Pearce, J.A., Harris, N.B.W., Tindle, A.G., 1984. Trace element discrimination diagrams for the tectonic interpretation of granitic rocks. Journal of Petrology 25, 956–983.
Pearce, J.A., Stern, R.J., Bloomer, S.H., Fryer, P., 2005. Geochemical mapping of the Mariana arc-basin system: implications for the nature and distribution of subduction components. Geochemistry, Geophysics, Geosystems 6, Q07006. http://dx.doi.org/10.1029/2004GC000895.
Pindell, J.L., Barrett, S.F., 1990. Geological evolution of the Caribbean region: a plate tectonic perspective. In: Dengo, G., Case, J.E. (Eds.), The Caribbean Region, the Geology of North America volume H. Geological Society of America, pp. 405–432.
Pindell, J., Maresch, W.V., Martens, U., Stanek, K., 2011. The Greater Antillean Arc: Early Cretaceous origin and proposed relationship to Central American subduction mélanges: implications for models of Caribbean evolution. International Geology Review 54, 131–143.
Reagan, M.K., Ishiuka, O., Stern, R.J., Kelley, K.A., Ohara, Y., Blichert-Toft, J., Bloomer, S.H., Cash, J., Fryer, P., Hanan, B.B., Hickey-Vargas, R., Ishii, T., Kimura, J.I., Peate, D.W., Rowe, M.C., Woods, M., 2010. Fore-arc basalts and subduction initiation in the Izu-Bonin–Mariana system. Geochemistry, Geophysics, Geosystems 11, Q03X12. http://dx.doi.org/10.1029/2009GC002871.
Reagan, M.K., McClelland, W.C., Guillaume, G., Goff, K.R., Peate, D.W., Ohara, Y., Stern, R.J., 2013. The geology of the southern Mariana fore-arc crust: implications for the scale of Eocene volcanism in the western Pacific. Earth and Planetary Science Letters 380, 41–51.
Révillon, S., Arndt, N.T., Chauvel, C., Hallot, E., 2000a. Geochemical study of ultramafic volcanic and plutonic rocks from Gorgona Island, Colombia: the plumbing system of an oceanic plateau. Journal of Petrology 41, 1127–1153.
Révillon, S., Hallot, E., Arndt, N.T., Chauvel, C., Duncan, R.A., 2000b. A complex history for the Caribbean Plateau: petrology, geochemistry, and geomorphology of the Beata Ridge, South Hispaniola. Journal of Geology 108, 641–666.
Rojas-Agramonet, Y., Kröner, A., García-Casco, A., Somin, M., Iturralde-Vinent, J., Wingate, D., Liu, Y., 2011. Timing and evolution of Cretaceous Island Arc magmatism in Central Cuba: implications for the history of arc systems in the Northwestern Caribbean. Journal of Geology 119, 619–640.
Rudnick, R.L., Gao, S., 2003. Composition of the continental crust. In: Rudnick, R.L., Holland, H.D., Turekian, K.K. (Eds.), Treatise on Geochemistry. 3, pp. 1–64.
Sano, T., Shimizu, K., Ishikawa, A., Senda, R., Chang, Q., Kimura, J.-I., Widdowson, M., Sager, W.W., 2012. Variety and origin of magmas on Shatsky Rise, northwest Pacific Ocean. Geochemistry, Geophysics, Geosystems 13, Q08010. http://dx.doi.org/10.1029/2012GC004235.
Sen, G., Hickey-Vargas, R., Waggoner, D.G., Maurrasse, F., 1988. Geochemistry of basalts from the Dumisseau Formation, southern Haiti: implications for the origin of the Caribbean Sea crust. Earth and Planetary Science Letters 87, 423–437.
Serrano, L., Ferrari, L., López Martínez, M., Maria Petrone, C., Jaramillo, C., 2011. An integrative geologic, geochronologic and geochemical study of Gorgona Island, Colombia: implications for the formation of the Caribbean Large Igneous Province. Earth and Planetary Science Letters 309, 324–336.
Shervais, J.W., 1982. Ti-V plots and the petrogenesis of modern and ophiolitic lavas. Earth and Planetary Science Letters 59, 110–118.
Sinton, C.W., Duncan, R.A., Denyer, P., 1997. Nicoya Peninsula, Costa Rica: a single suite of Caribbean oceanic plateau magmas. Journal of Geophysical Research 102, 507–515. http://dx.doi.org/10.1029/97JB00681.
Sinton, C.W., Duncan, R.A., Storey, M., Lewis, J., Estrada, J.J., 1998. An oceanic flood basalt province within the Caribbean plate. Earth and Planetary Science Letters 155, 221–235.
Sinton, C.W., Sigurdsson, H., Duncan, R.A., 2000. Geochronology and petrology of the igneous basement at the lower Nicaraguan Rise, Site 1001. Proceedings of the Ocean Drilling Program, Scientific Results, Leg 165. Ocean Drilling Program, Texas A&M University, College Station, Texas, pp. 233–236.
Smith, C.A., Sisson, V.B., Avé Lallemant, H.G., Copeland, P., 1999. Two contrasting pressure–temperature–time paths in the Villa de Cura blueschist belt, Venezuela: possible evidence for Late Cretaceous initiation of subduction in the Caribbean. Geological Society of America Bulletin 111, 831–848.
Spikings, R.A., Winkler, W., Hughes, R.A., Handler, R., 2005. Thermochronology of allochthonous terranes in Ecuador: unraveling the accretionary and post-accretionary history of the Northern Andes. Tectonophysics 399, 195–220. http://dx.doi.org/10.1016/j.tecto.2004.12.023.
Stern, R.J., 2004. Subduction initiation: spontaneous and induced. Earth and Planetary Science Letters 226, 275–292.
Stern, R.J., Reagan, M., Ishizuka, O., Ohara, Y., Whattam, S., 2012. To understand subduction initiation, study forearc crust: to understand forearc crust, study ophiolites. Lithosphere http://dx.doi.org/10.1130/L183.1.
Sun, S.S., McDonough, W.F., 1989. Chemical and isotopic systematic of oceanic basalts: implications for mantle composition and processes. In: Saunders, A.D., Norry, M.J. (Eds.), Magmatism in the Ocean Basins. Geological Society of London Special Publication. 42, pp. 313–345.
Tejada, M.L.G., Mahoney, J.J., Neal, C.R., Duncan, R.A., Petterson, M.G., 2002. Basement geochemistry and geochronology of Central Malaita, Solomon Islands, with implications for the origin and evolution of the Ontong Java Plateau. Journal of Petrology 43, 449–484.
Ueda, K., Gerya, T., Sobolev, S.V., 2008. Subduction initiation by thermal–chemical plumes: numerical studies. Physics of the Earth and Planetary Interiors 171, 296–312.
Vallejo, C., Spikings, R.A., Luzieux, L., Winkler, W., Chew, D., Page, L., 2006. The early interaction between the Caribbean Plateau and the NW South American plate. Terra Nova 18, 264–269.
Vallejo, C., Winkler, W., Spikings, R.A., Luziuex, L., Heller, F., Bussy, F., 2009. Mode and timing terrane accretion in the forearc of the Andes in Ecuador. In: Kay, S.M., Ramos, V.A., Dickinson, W.R. (Eds.), Backbone of the Americas: shallow subduction, plateau uplift, and ridge and terrane collision. Geological Society of America Memoir. 204, pp. 197–216. http://dx.doi.org/10.1130/2009.1204.
van der Lelij, R., Spikings, R.A., Kerr, A.C., Kounov, A., Cosca, M., Chew, D., Villagomez, D., 2010. Thermochronology and tectonics of the Leeward Antilles: evolution of the southern Caribbean Plate boundary. Tectonics 29, TC6003. http://dx.doi.org/10.1029/2009TC002654.
van Hinsbergen, D.J.J., Iturralde-Vinent, M.A., van Geffen, P.W.G., García-Casco, A., van Benthem, S., 2009. Structure of the accretionary prism, and the evolution of the Paleogene northern Caribbean subduction zone in the region of Camagüey, Cuba. Journal of Structural Geology 31, 1130–1144.
Vaughan, A.P.M., 1995. Circum-Pacific mid-Cretaceous deformation and uplift: a superplume-related event? Geology 23, 491–494.
Villagómez, D., Spikings, R., Magna, T., Kammer, A., Winkler, W., Beltrán, A., 2011. Geochronology, geochemistry and tectonic evolution of the Western and Central cordilleras of Colombia. Lithos 125, 875–896.
Walker, R.J., Storey, M.J., Kerr, A.C., Tarney, J., Arndt, N.T., 1999. Implications of ^{187}Os isotopic heterogeneities in a mantle plume: evidence from Gorgona Island and Curacao. Geochimica et Cosmochimica Acta 63, 13–728.
Wang, X.-C., Li, X.-H., Li, W.-X., Li, Z.-X., 2009. Variable involvements of mantle plumes in the genesis of mid-Neoproterozoic basaltic rocks in South China: a review. Gondwana Research 15, 381–395.

Weber, M.B.I., Cardona, A., Paniagua, F., Cordani, U., Sepúlveda, L., Wilson, R., 2009. The Cabo de la Vela Mafic–Ultramafic Complex, Northeastern Colombian Caribbean region: a record of multistage evolution of a late Cretaceous intra-oceanic arc. In: James, K.H., Lorente, M.A., Pindell, J.L. (Eds.), The origin and evolution of the Caribbean Plate. Geological Society of London Special Publications. 328, pp. 547–566.
Wegner, W., Wörner, G., Harmon, R.S., Jicha, B.R., 2011. Magmatic history and evolution of the Central American land bridge in Panama since Cretaceous time. Geological Society of America Bulletin 123, 703–734.
Wells, R.E., Engebretson, D.C., Snavely Jr., P.D., Coe, R.S., 1984. Oregon plate motions and the volcano-tectonic evolution of western Oregon and Washington. Tectonics 3, 275–284.
Whattam, S.A., 2009. Arc-continent collisional orogenesis in the SW Pacific and the nature, source and correlation of emplaced ophiolitic nappe components. Lithos 113, 88–114.
Whattam, S.A., Stern, R.J., 2011. The 'subduction initiation rule': a key for linking ophiolites, intra-oceanic forearcs, and subduction initiation. Contributions to Mineralogy and Petrology 62, 1031–1045. http://dx.doi.org/10.1007/s00410-011-0638-z.
White, R.V., Tarney, J., Kerr, A.C., Saunders, A.D., Kempton, P.D., Pringle, M.S., Klaver, G.T., 1999. Modification of an oceanic plateau, Aruba, Dutch Caribbean: implications for the generation of continental crust. Lithos 46, 43–68. http://dx.doi.org/10.1016/S0024-4937(98)00061-9.
White, W.M., McBirney, A.R., Duncan, R.A., 1993. Petrology and geochemistry of the Galapagos Islands: portrait of a pathological mantle plume. Journal of Geophysical Research 98 (B11), 19533–19563.
Wiedmann, J., 1978. Ammonites from the CLF, Curaçao, Caribbean. Geologie & Mijnbouw 57, 361–364.
Wörner, G., Harmon, R.S., Wegner, W., 2009. In: Kay, S.M., Ramos, V.A., Dickinson, W.R. (Eds.), Backbone of the Americas: shallow subduction, plateau uplift, and ridge and terrane collision. Geological Society of America Memoir. 204, pp. 183–196. http://dx.doi.org/10.1130/2009.1204.
Wright, J.E., Wyld, S.J., 2011. Late Cretaceous subduction initiation on the eastern margin of Caribbean–Colombian oceanic plateau: one great arc of the Caribbean (?). Geosphere 7, 468–493. http://dx.doi.org/10.1130/GES00577.1.
Zimmer, M., Plank, T., Hauri, E.H., Yogodzinski, G.M., Stelling, P., Larsen, J., Singer, B., Jicha, B., Mandeville, C., Nye, C.J., 2010. The role of water in generating the calc-alkaline trend: new volatile data for Aleutian magmas and a new tholeiitic index. Journal of Petrology 51, 2411–2444.
Zindler, A., Hart, S., 1986. Chemical geodynamics. Annual Review of Earth and Planetary Sciences 14, 493–571.

Scott A. Whattam holds a BSc from Carleton University, Canada and a PhD from the University of Hong Kong, SAR China. He is an Associate Professor of Petrology at Korea University (Seoul, Republic of Korea). He held post-doctoral positions at Seoul National University (Republic of Korea), Rutgers University (US) and the Smithsonian Tropical Research Institute (Panama City, Panama). His research interests include understanding the relation between ophiolites, forearc crust and subduction initiation; and cosmochemistry and early solar system studies. His land- and sea-based research has been conducted on ophiolite and arc-related terranes in the SW Pacific, North Pacific, East Asia and Central America. His NASA-funded, laboratory-based experimental petrology studies have focused on constraining the thermal and temporal evolution of earliest solar nebula components such as ferromagnesian silicate chondrules and Ca–Al-rich refractory inclusions. He has served on the Editorial Board of International Geology Review since July 2013.

Robert J. Stern is a Professor of Geosciences at the University of Texas at Dallas, where he has been a member of the faculty since 1982. He received his undergraduate training at the University of California at Davis, and his PhD at the Scripps Institute of Oceanography at UC San Diego. He carried out post-doctoral studies at the Department of Terrestrial Magnetism, Carnegie Institution of Washington, and he has been a visiting scholar at Stanford University, Caltech and ETH. His research focuses on understanding how subduction zones operate, how convergent margin magmatic systems form and evolve, how the continental crust is generated and destroyed, how new subduction zones form, and when Plate Tectonics began. This research agenda requires studies on land and at sea and many scientific collaborations. Information about his research can be found on Google Scholar. He is the Editor-in-Chief of International Geology Review.